8-4-2022

Exoskeletal predator defenses of juvenile California spiny lobsters (Panulirus interruptus) are affected by fluctuating ocean acidification-like conditions

Kaitlyn B. Lowder
Marine Biology Research Division

Maya S. deVries
San Jose State University, maya.devries@sjsu.edu

Ruan Hattingh
Geosciences Research Division

James M.D. Day
Geosciences Research Division

Andreas J. Andersson
Geosciences Research Division

See next page for additional authors

Recommended Citation

Kaitlyn B. Lowder, Maya S. deVries, Ruan Hattingh, James M.D. Day, Andreas J. Andersson, Phillip J. Zerofski, and Jennifer R.A. Taylor. "Exoskeletal predator defenses of juvenile California spiny lobsters (Panulirus interruptus) are affected by fluctuating ocean acidification-like conditions" *Frontiers in Marine Science* (2022). https://doi.org/10.3389/fmars.2022.909017

frontiers | Frontiers in Marine Science

TYPE Original Research
PUBLISHED 04 August 2022
DOI 10.3389/fmars.2022.909017

OPEN ACCESS

EDITED BY:
Gary H. Dickinson,
The College of New Jersey,
United States

REVIEWED BY:
Joseph Kunkel,
University of Massachusetts Amherst,
United States
Aaron Ninokawa,
Friday Harbor Laboratories, College of the Environment, University of Washington, United States

*CORRESPONDENCE:
Kaitlyn B. Lowder
kaitlyn.b.lowder@gmail.com
Jennifer R. A. Taylor
j3taylor@ucsd.edu

†PRESENT ADDRESS:
Kaitlyn B. Lowder,
The Ocean Foundation, Washington, DC, United States

SPECIALTY SECTION:
This article was submitted to Marine Molecular Biology and Ecology, a section of the journal Frontiers in Marine Science

RECEIVED: 31 March 2022
ACCEPTED: 28 June 2022
PUBLISHED: 04 August 2022

CITATION:
Lowder KB, deVries MS, Hattingh R, Day JMD, Andersson AJ, Zerofski PJ and Taylor JRA (2022) Exoskeletal predator defenses of juvenile California spiny lobsters (*Panulirus interruptus*) are affected by fluctuating ocean acidification-like conditions. *Front. Mar. Sci.* 9:909017. 10.3389/fmars.2022.909017

Exoskeletal predator defenses of juvenile California spiny lobsters (*Panulirus interruptus*) are affected by fluctuating ocean acidification-like conditions

Kaitlyn B. Lowder[1*†], Maya S. deVries[2], Ruan Hattingh[3], James M. D. Day[3], Andreas J. Andersson[3], Phillip J. Zerofski[1] and Jennifer R. A. Taylor[1*]

[1]Marine Biology Research Division, Scripps Institution of Oceanography, University of California, San Diego, La Jolla, CA, United States, [2]Department of Biological Sciences, San José State University, San Jose, CA, United States, [3]Geosciences Research Division, Scripps Institution of Oceanography, University of California, San Diego, La Jolla, CA, United States

Spiny lobsters rely on multiple biomineralized exoskeletal predator defenses that may be sensitive to ocean acidification (OA). Compromised mechanical integrity of these defensive structures may tilt predator-prey outcomes, leading to increased mortality in the lobsters' environment. Here, we tested the effects of OA-like conditions on the mechanical integrity of selected exoskeletal defenses of juvenile California spiny lobster, *Panulirus interruptus*. Young spiny lobsters reside in kelp forests with dynamic carbonate chemistry due to local metabolism and photosynthesis as well as seasonal upwelling, yielding daily and seasonal fluctuations in pH. Lobsters were exposed to a series of stable and diurnally fluctuating reduced pH conditions for three months (ambient pH/stable, 7.97; reduced pH/stable 7.67; reduced pH with low fluctuations, 7.67 ± 0.05; reduced pH with high fluctuations, 7.67 ± 0.10), after which we examined the intermolt composition (Ca and Mg content), ultrastructure (cuticle and layer thickness), and mechanical properties (hardness and stiffness) of selected exoskeletal predator defenses. Cuticle ultrastructure was consistently robust to pH conditions, while mineralization and mechanical properties were variable. Notably, the carapace was less mineralized under both reduced pH treatments with fluctuations, but with no effect on material properties, and the rostral horn had lower hardness in reduced/high fluctuating conditions without a corresponding difference in mineralization. Antennal flexural stiffness was lower in reduced, stable pH conditions compared to the reduced pH treatment with high fluctuations and not correlated with changes in cuticle structure or mineralization. These results demonstrate a complex relationship between mineralization and mechanical properties of the exoskeleton under changing ocean chemistry, and that fluctuating reduced pH conditions can induce responses not observed under the stable reduced pH conditions often used in OA research. Furthermore, this study shows that some juvenile California spiny lobster exoskeletal defenses are responsive to changes in

ocean carbonate chemistry, even during the intermolt period, in ways that can potentially increase susceptibility to predation among this critical life stage.

KEYWORDS

crustacean, ocean acidification, predator defense, mechanical properties, exoskeleton, decapod

Introduction

Marine invertebrates possess a diverse array of weapons and defense structures that use biomineralization to confer sufficient hardness and stiffness for optimal function. Structures spanning spines, plates, claws, mandibles, antennae, raptorial appendages, shells, and exoskeletons all have hierarchical structural design elements fortified with minerals, such as calcium carbonates and calcium phosphates, that help produce the material properties for a specific function. Yet, biomineralization, particularly calcification, in marine organisms is demonstrably sensitive to ocean acidification-like reduced pH/high pCO_2 conditions (Kroeker et al., 2010). Most invertebrates with calcified structures experience reductions in mineral content (Chan and Connolly, 2013; Kroeker et al., 2013; Davis et al., 2021) under reduced pH/high pCO_2 exposure due to lowered carbonate ion concentration and carbonate mineral saturation state. In contrast, some crustacean species experience increases in calcification (McDonald et al., 2009; Long et al., 2013; Taylor et al., 2015; deVries et al., 2016; Glandon et al., 2018), which is potentially accomplished by drawing upon bicarbonate accumulated for acid-base regulation (Truchot, 1979; Pane and Barry, 2007; Spicer et al., 2007; Knapp et al., 2015; Whiteley et al., 2018). The degree of mineralization is strongly linked with material properties, whereby greater mineral content corresponds to greater stiffness and brittleness (Currey, 1984). Thus, disruptions to the biomineralization process under ocean acidification (OA) conditions, resulting in either decreases or increases to calcification, have the potential to alter the mechanical integrity of defense structures and ultimately the potential outcomes of predator-prey interactions in future ocean conditions.

OA research often targets biomineralization responses, but rarely are the effects on material properties and mechanical functioning, which are consequential for survival during predator-prey interactions, studied concurrently. Reduced calcification is generally purported to have negative consequences on material properties and mechanical efficiency. This is exemplified by reduced calcification corresponding with lower stem stiffness in a calcified green alga and decreased shell elasticity in a Mediterranean top snail, both studied at CO_2 seep sites (Newcomb et al., 2015; Duquette et al., 2017), and decreased abalone shell fracture toughness concurrent with reductions in shell mineralization and thickness under reduced pH conditions (Auzoux-Bordenave et al., 2020; Avignon et al., 2020). Increased calcification, however, can also create weaker barnacle shell wall plates (McDonald et al., 2009) due to increased brittleness. In mantis shrimp, exoskeletal hardness and stiffness remained the same despite increases to Mg content (deVries et al., 2016). Altered mineralization, either through increases or decreases, has the potential to disrupt the material properties and mechanical efficiency of organism structures, but the thresholds for these effects are likely specific to structures and species (Siegel et al., 2022). As such, there is still much to learn about the relationship between changes to material composition and the degree to which the material is compromised. Unraveling this relationship will help inform how single-species responses can be inferred to impact species interactions, such as predator-prey encounters.

A better understanding of potential impacts is especially needed for crustaceans, which have generally garnered less OA research attention than other marine calcifiers (Whiteley, 2011; Siegel et al., 2022), but have an exoskeleton that is complex, multifunctional, and highly variable within a single individual. The decapod crustacean exoskeleton is heterogenous and comprised of mineral, usually in the form of calcite, magnesian calcite, amorphous calcium carbonate, and sometimes calcium phosphate, that is embedded among lamellae of sugars and protein, which stack to form the distinct layers of the epicuticle, exocuticle, and endocuticle (Travis, 1963; Huner et al., 1979; Vigh and Dendinger, 1982; Addadi et al., 2003; Dillaman et al., 2005; Boßelmann et al., 2007; Kunkel et al., 2012). Within the exocuticle and endocuticle, layer thickness, lamellae stacking density, and mineral composition can all be adjusted to produce a spectrum of material properties that support a range of exoskeleton functions (Raabe et al., 2005; Chen et al., 2008). Crustaceans can construct exoskeletal regions with specificity to meet functional demands (Melnick et al., 1996; Dutil et al., 2000; Chen et al., 2008) and likely have complex responses to OA-like conditions (Siegel et al., 2022).

Exoskeleton versatility is exemplified in the California spiny lobster, *Panulirus interruptus*, which begin living in coastal kelp forests as juveniles and use their exoskeleton in a suite of defenses against predators such as octopus, eels, and large fish, particularly the California sheephead, *Semicossyphus pulcher* (Lindberg, 1955; Loflen and Hovel, 2010; Higgins et al., 2018). One of the first strategies that spiny lobsters can employ to avoid harm is using the rostral horns to lock onto the roof of a rocky

shelter to avoid expulsion (Lindberg, 1955). Another option is to use their long, spiny antennae to push against predators, keeping the bulk of their body a safe distance away (Barshaw et al., 2003; Briones-Fourzán et al., 2006). As a last line of defense, the carapace is coated in flattened spines that likely enhance pierce-resistance (Tarsitano et al., 2006). Each of these defense behaviors are dependent on the exoskeleton being sufficiently stiff, hard, and strong under their different loading regimes, and their distinct composition and structure affords them the proper mechanical properties to achieve their function (Lowder, 2019). These defense structures, however, may be differentially vulnerable to the impacts of changing carbonate chemistry and therefore yield greater insight into the variable effects of OA on the structure-property relationships of calcified materials.

Understanding the impacts on spiny lobsters is not only complicated by the variability in their exoskeleton, but also by the variability in their environment. Spiny lobsters, like a number of other coastal organisms, live in dynamic environments that may shape their response to changing ocean conditions. Juvenile *P. interruptus* spend two to three years in shallow eelgrass or kelp environments (Engle, 1979), where they must be able to successfully exercise their full range of predator defense strategies while contending with diurnal changes in their environment (Frieder et al., 2012). In coastal environments, carbonate chemistry fluctuates diurnally, tidally, and seasonally (Johnson et al., 2013), producing variable conditions to which organisms in these habitats are subjected. In environments dominated by a large biomass of photosynthetic organisms, such as kelp forests or seagrass meadows, daily ranges of pH may be as great as the decrease in pH expected over the next century, 0.3-0.4 units (Frieder et al., 2012; Challener et al., 2015; James et al., 2019) driven in part by the uptake of CO_2 *via* photosynthesis during the day and organismal respiration at night. These ranges can be even greater than 1 unit (Semesi et al., 2009) depending on currents, tides, depth, and community composition (Hofmann et al., 2011; Page et al., 2016; Silbiger and Sorte, 2018). In addition, in coastal regions where seasonal upwelling is prominent, such as the U.S. West Coast, further decreases in near-shore pH may occur owing to intrusion of deep seawater with high CO_2 and low pH (Takeshita et al., 2015; Chan et al., 2017; Kekuewa et al., 2020).

For organisms that inhabit dynamic environments, the exposure to a range of conditions has potentially led to a degree of adaptation that may be beneficial as ocean carbonate chemistry continues to change. A growing, but still limited, number of studies have imposed fluctuations around low and high pH setpoints and discovered varied responses. For example, fluctuating pH conditions may ameliorate some or all of the negative growth and sensory impacts observed at stable reduced pH in pink salmon (Ou et al., 2015) and coral reef fish, where it is hypothesized to help prevent physiological changes in the brain (Jarrold et al., 2017). *Mytilus edulis* mussels take advantage of higher pH during the day to increase calcification rates, lessening the overall negative impact to calcification (Wahl et al., 2018), while *Mytilus galloprovincialis* veligers experiencing fluctuating reduced pH did not experience the same reductions in shell length that those in stable reduced pH did (Frieder et al., 2014). Yet, in some organisms, fluctuating pH conditions either have no discernable effect from stable reduced pH conditions (Clark and Gobler, 2016), or they appear to increase stress, producing more negative responses than stable reduced pH conditions alone (Alenius and Munguia, 2012; Mangan et al., 2017; Onitsuka et al., 2017; Johnson et al., 2019). Thus, to establish realistic impacts on organisms like the California spiny lobster, it is important to incorporate the natural fluctuating conditions of their habitat into OA experiments (Andersson and Mackenzie, 2012; McElhany and Busch, 2013; Andersson et al., 2015).

In this study, we exposed juvenile California spiny lobsters, *Panulirus interruptus*, to stable and fluctuating high pCO_2/reduced pH conditions that mimic their current and future habitat and examined the integrity of their predator defenses. Specifically, we examined the rostral horns, antennae, and carapace for elemental composition (Ca and Mg content), structure (cuticle and layer thickness), and material properties (hardness and stiffness) (Figure 1). We hypothesized that lobsters under low, stable pH conditions would have relatively higher exoskeleton mineralization than those in ambient conditions, resulting in altered mechanical properties, while these effects would be lessened in the fluctuating reduced pH conditions due to a respite from constant reduced pH conditions. Alternatively, the fluctuating reduced pH conditions may exceed potential pH thresholds, eliciting the same or exacerbated responses. We also hypothesized that the magnitude of response would vary across defensive structures due to localized control and functional specificity.

Methods

Animal collection

Sixty-four juvenile lobsters were collected from offshore La Jolla, San Diego, CA over the course of six days in October 2016. Commercial lobster traps were modified with smaller mesh and set at depths of 8.5 to 15.2 m. Lobsters were transported to the experimental aquarium at Scripps Institution of Oceanography (SIO) within 2.5 hours of collection and placed in flow-through seawater pumped from the Scripps Pier, approximately 2 km northeast from the site of collection.

Experimental design

The experimental ocean acidification system consisted of four 81 L header tanks that each received filtered seawater pumped from the SIO pier (3-4 m depth, 300 m offshore) at ambient pH (7.97 ± 0.03), pCO_2 (464 ± 39 µatm), and salinity (33.4 ± 0.2 PSU) (mean ± s.d. during the experimental period). A mix of chilled

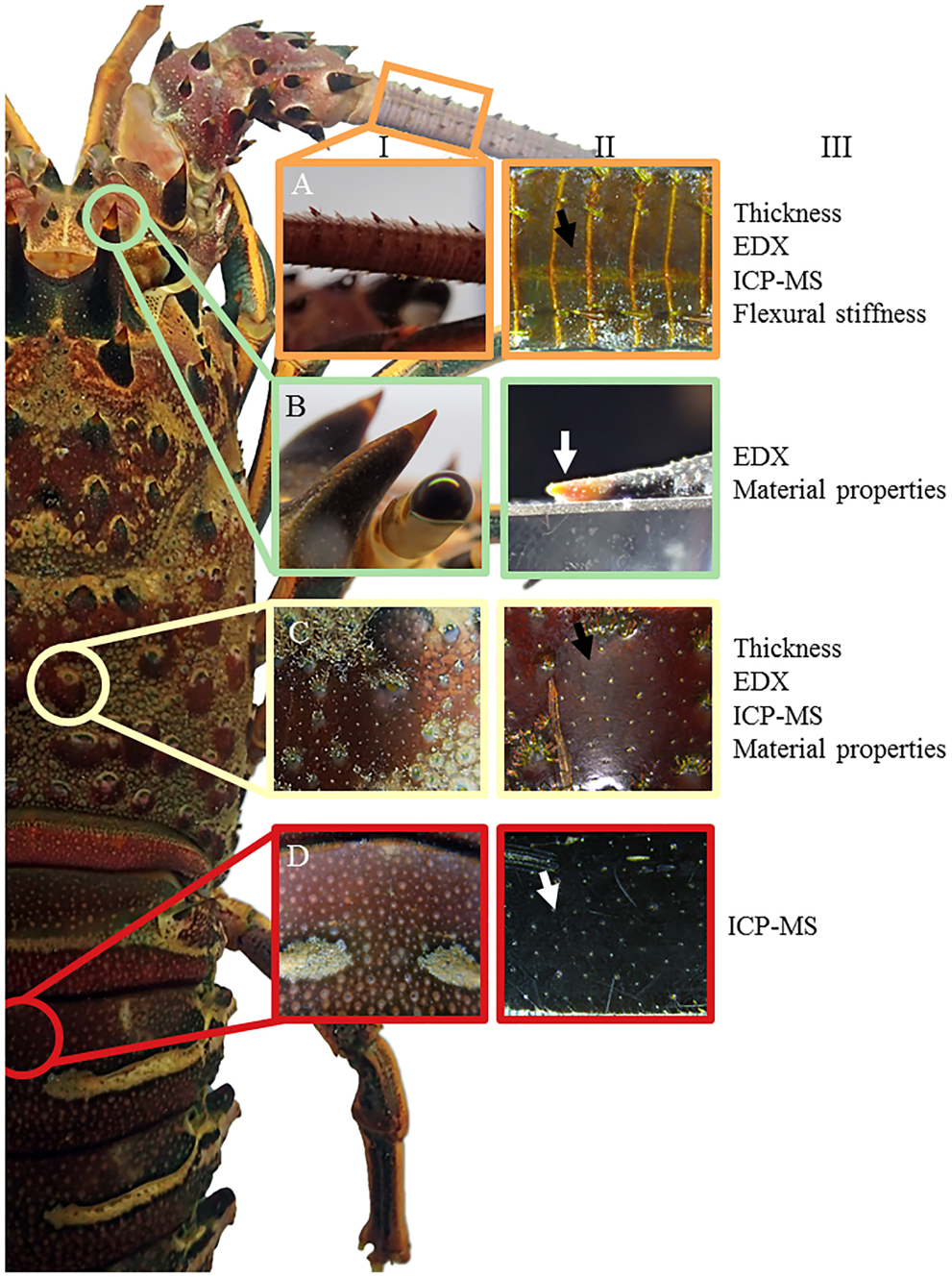

FIGURE 1
Exoskeletal defense structures of *Panulirus interruptus*. **(A)** antenna, **(B)** horn tip, **(C)** carapace spine, **(D)** abdominal segment in image columns I and II. The analyses performed for each structure are listed in column III. Arrows indicate areas where nanoindentation was performed normal to the surface. The horn tip in B-II is affixed to an aluminum block for nanoindentation.

and ambient temperature seawater was fed into the header tanks, which were maintained at a stable 16.5 ± 0.6°C with the aid of heaters. Two 1585 GPH aquarium powerheads were placed in each header tank to ensure adequate mixing.

One header tank was kept at ambient pH to provide the control treatment while the three others were adjusted for high pCO_2/low pH treatments. One treatment was adjusted to a stable pH of 7.7, congruent with current predictions for decreases in global ocean surface pH values of 0.3 pH units by the year 2100 (IPCC, 2014). pH levels as low as 7.77 have been observed at 10 m in the habitat of spiny lobsters during upwelling seasons (Kekuewa et al., 2020). In the kelp forest less than 1000 m from

the site of lobster collection, pH was found to average 8.05 units at 7 m depth with minima around 7.8 during a springtime period of observation (Frieder et al., 2012). The two other treatments were set to fluctuate around this reduced pH, but to different degrees. The reduced/low fluctuating pH treatment was set to 7.7 ± 0.05 (total range: 7.65-7.75) pH units based on published measurements of southern California kelp forest diurnal pH variations, which depend upon tide, season, and weather conditions, and which are approximately 0.1 pH units on average (Frieder et al., 2012; Kapsenberg and Hofmann, 2016). The reduced/high fluctuating pH treatment was set to 7.7 ± 0.10 (total range: 7.6-7.8) pH units, which mimics future diurnal fluctuations, calculated in CO_2Sys for decreases in buffering capacity associated with higher anthropogenic pCO_2 values and thus larger pH swings assuming the same autotrophic forcing of DIC (Pierrot et al., 2006). For both of the fluctuating treatments, high pH values were held stable for approximately 10 hours to match daylight (and photosynthesis) hours at the time of the experiment. Nighttime low pH values were held stable for 12 hours. pH was set at a midpoint value for one hour between each of these highs and lows as a transition period.

Experimental pH conditions were achieved by bubbling 100% CO_2 into the three treatment header tanks and were controlled by an Apex Lite aquarium controller with Apex Neptune pH and temperature probes (0.01 pH accuracy; temperature accuracy 0.1°C, Neptune Systems, Morgan Hill, CA, USA). pH and temperature of the header tanks were logged every 10 minutes throughout the duration of the experiment. The Apex pH probes were calibrated prior to the experimental period, but because stability and not accuracy was desired, they were not calibrated again.

Each header tank supplied flow-through seawater separately to 16 experimental tanks (8.4 L) that were randomly intermixed in the experimental area. Each experimental tank contained a single lobster, for a combined total of 64 individuals. Experimental water parameters were gradually altered over the course of three days to minimize potential acute stress. Once the targeted water parameters were reached, the experiment was run for 102 days.

Water chemistry

Daily readings of pH and temperature were taken from each lobster tank using a portable probe (HQ40d, probe PHC201, precision 0.01 pH, 0.1 temperature, Hach, Loveland, CO, USA) as a method of high-frequency measurements in between discrete carbonate chemistry water sample measurements (Figure S1). This probe was calibrated with NBS buffer solutions (Fisher Scientific, Fair Lawn, NJ, USA) approximately every three weeks to control its slow drift. Daily readings were taken at consistent times during the daytime to capture the high value in the fluctuating treatments. Calculated pH from discrete water samples (see below) was averaged for each sampling period and used to correct the portable probe values to pH_{total}. Each water sampling round corresponded to one calibration period of the portable probe.

Nighttime pH was checked using two methods to confirm that stable treatments were constant and that target fluctuations were achieved and consistent. In addition to four probes constantly monitoring and logging header tank pH, two additional Neptune Apex electrodes were rotated between random lobster tanks once per day and recorded pH every 10 minutes over the course of each 24-hour period. Nighttime pH in the fluctuating treatments was recorded to be 0.11 ± 0.02 (n = 54) and 0.21 ± 0.03 (n = 46) pH units lower than daytime pH, consistent with our targeted values. Periodic measurements of nighttime pH with the handheld probe (n=8) were in agreement with the readings of the Apex probes.

Discrete samples were collected for water chemistry analysis four times from three randomized lobster tanks per treatment over the experimental period (48 samples total). Samples were collected in 500 mL Pyrex glass bottles and poisoned with 120 µL of a saturated solution of $HgCl_2$ in accordance with standard operating procedures (Dickson et al., 2007). Each water sample was analyzed for total alkalinity (A_T) by potentiometric acid titration (0.1 N HCl) using an 876 Dosimat (Metrohm, Riverview, Florida, USA) and pH electrode (Ecotrode Plus, Metrohm, Riverview, Florida, USA) and for dissolved inorganic carbon (DIC) using an AIRICA system (Marianda, Kiel, Germany) with integrated infrared CO_2 analyzer (Li-COR 7000, Li-COR, Lincoln, Nebraska, USA). Certified reference material (CRM) provided by the Dickson laboratory at SIO were used to verify the accuracy and precision, both to ± 1–4 µmol kg^{-1}, before and after measuring samples as well as between every five samples for DIC and ten for A_T. Other parameters of the carbonate system were calculated using CO_2Sys 25.06 (Pierrot et al., 2006) (**Table 1**). For calculations, dissociation constants of K_1, K_2 were from Mehrbach et al., 1973, refit by Dickson and Millero, 1987. The HSO_4^- constant was from Dickson, 1990 and the [B]T value was from Uppström, 1974.

Survival, molting, and growth

Lobsters were fed equal amounts of squid five days per week in excess, with remaining food removed daily. Tanks were checked daily for deaths and molting events; exuviae were promptly removed to prevent fouling and consumption. Growth was recorded at the start and end of the experiment by weighing damp lobsters in air after removal from tanks and allowing excess water to run off. Carapace length was measured from the notch at the base of the rostral horns to the posterior edge of the carapace at the dorsal midline. Initial size ranged from 43.5 to 58.5 mm carapace length (CL) and 75.4 to 198.2 g. Of the 64 lobsters, 20 were male and 44 were female, and 30% showed at least some physical indications of sexual maturity (e.g., softened sternal plates and enlarged testes identified during dissection). Carapace

TABLE 1 Water parameters during the experimental period as mean ± sd.

Treatment	Daytime pH (total)	Daily range of pH	Mean pH (total)	Temp (°C)	DIC (µmol/kg SW)	TA (µmol/kg SW)	pCO_2 (µatm)	HCO_3^- (µmol/kg SW)	Ω Calcite
Ambient/ stable (7.97)	7.97 ± 0.03 [1329]	0.01 ± 0.01 [49]	7.97	16.5 ± 0.6 [1560]	2030 ± 16 [12]	2219 ± 10 [12]	464 ± 39 [12]	1873 ± 30 [12]	3.37 ± 0.32 [12]
Reduced/ stable (7.67)	7.67 ± 0.04 [1350]	0.01 ± 0.02 [50]	7.67	16.6 ± 0.6 [1569]	2136 ± 11 [12]	2218 ± 9 [12]	978 ± 53 [12]	2023 ± 13 [12]	1.90 ± 0.15 [12]
Reduced/ low fluctuating (7.67 ± 0.05)	7.72 ± 0.03 [1317]	0.11 ± 0.02 [54]	7.67	16.4 ± 0.5 [1662]	2124 ± 11 [12]	2219 ± 8 [12]	863 ± 71 [12]	2008 ± 14 [12]	2.06 ± 0.14 [12]
Reduced/ high fluctuating (7.67 ± 0.10)	7.77 ± 0.03 [1333]	0.21 ± 0.03 [46]	7.67	16.4 ± 0.7 [1667]	2103 ± 12 [12]	2219 ± 8 [12]	751 ± 52 [12]	1979 ± 17 [12]	2.34 ± 0.20 [12]

Values in brackets indicate the sample size. pH is calculated by applying the offset between discrete water samples and portable probe readings to the daily probe readings. Daily ranges of pH are calculated from two Apex probes that were rotated between lobster tanks daily. The mean pH for each treatment was determined as the midpoint between mean daytime and nighttime pH. Temperature is from daily portable probe readings. DIC and TA are directly measured from discrete water samples, while pCO_2, HCO_3^-, and calcite saturation state are all calculated from discrete water samples using CO_2Sys; these values reflect daytime conditions. Nighttime pH values may be inferred from the difference between the daytime pH and the daily range.

length and sex were used to assign individuals to each treatment so that these factors were evenly distributed.

Cuticle structure and elemental composition

At the end of the experiment, lobsters were anesthetized by brief placement in a -20°C freezer and then sacrificed by piercing the exoskeleton and tissue between the rostral horns with a ceramic knife. Samples of cuticle were dissected by cutting ~ 0.75 x 0.75 cm^2 around a consistent carapace spine located below the cephalothorax line, a 0.5 x 1.5 cm^2 section of the antennae 1 cm above the posterior base on the dorsal side, and around the base of the rostral horn. Each cuticle sample was rinsed with DI water and allowed to air dry. Samples were then freeze-fractured with liquid nitrogen so that an orthogonal cross-section was produced and critical-point dried (AutoSamdri 815 Series A, Tousimis, Rockville, MD, USA) before being mounted on a 90-degree SEM tip and sputter-coated with iridium.

Cross-sections of these cuticle samples were examined with ultra-high-resolution scanning electron microscopy under high vacuum (XL30 SFEG with Sirion column and Apreo LoVac, FEI, Hillsboro, OR, USA with Oxford X-MAX 80 EDS detector, Concord, MA, USA) at 10 or 20 kV. One to two samples each of the carapace spine and antenna from individual lobsters were imaged and measured for the total cuticle thickness (epicuticle, exocuticle, and endocuticle), as well as thickness of the individual exo- and endocuticle layers, which were differentiated by the abrupt change in lamellae stacking density (Figure S3). The rostral horn has an unusual structure, consisting of only two layers: an inner region, that we will refer to as the core, and an outer layer that we will refer to as the outer ring (Lowder, 2019). Layer thickness (and the total thickness) for which the sample did not produce a clean cross section, most commonly observed as a flaky and uneven endocuticle, were not included in analyses (n=0-2 per layer per treatment).

Elemental composition of cuticle samples was quantified using both energy-dispersive x-ray spectroscopy (EDX) and inductively coupled plasma mass spectrometry (ICP-MS). The spatial resolution of EDX enabled elemental sampling of the surface of exocuticle and endocuticle layers separately, whereas ICP-MS provided precise quantification of elements present in the whole volume of cuticle sample. EDX was measured with two machines (XL30 SFEG with Sirion column and Apreo LoVac, FEI, Hillsboro, OR, USA with Oxford X-MAX 80 EDS detector, Concord, MA, USA) at 20 kV acceleration voltage. Spectra were taken on the cross-sectional surface of the exocuticle and the endocuticle layers of the carapace spine and antenna base and the core and outer ring of the horn tip. Eleven elements were consistently present in varying amounts: C, N, O, Ca, Mg, Na, Al, P, Si, S, and Cl. The amount of Ca and Mg were expressed as weight percent (% wt) relative to the other nine elements.

Inductively-coupled plasma mass spectrometry (ICP-MS) was performed on cuticle samples at the Scripps Isotope Geochemistry Laboratory (SIGL) for a precise quantification of elements. The carapace spine was air-dried and then trimmed so only the spine remained with no setae, and the abdominal segment was cut as a 1 x 1 cm^2 from the center of the second abdominal segment and air-dried. Samples were weighed and placed in Teflon vials for digestion with 0.5 ml of concentrated Teflon-distilled (TD) nitric acid (HNO_3) on a hotplate at 100°C for >24 h. Samples were dried down and diluted by a factor of 4000 with 2% TD HNO_3 before being transferred to pre-cleaned centrifuge tubes for analysis. Samples were doped with an indium

solution to monitor instrumental drift. Measurements were done using a ThermoScientific iCAPq c ICP-MS (Thermo Fisher Scientific GmbH, Bremen, Germany) in standard mode. Masses of Mg and Ca were sequentially measured for 30 ratios, resulting in internal precision of <2% (2 s.d.). Elements were corrected for total mole fraction. Total procedural blanks represented <0.3% of the measurement for Mg and Ca. Raw data were corrected offline for instrument background and drift. Samples were bracketed by internal standards of crab carapace (n=3), which allowed for calculation of absolute values. The standards yielded external precision of 2% and 3% for Mg and Ca, respectively. We targeted the following isotopes: ^{10}B, ^{25}Mg, ^{26}Mg, ^{27}Al, ^{29}Si, ^{31}P, ^{43}Ca, ^{48}Ca, ^{54}Fe, ^{57}Fe, ^{65}Cu, ^{66}Zn, ^{86}Sr, ^{111}Cd, ^{137}Ba, ^{208}Pb, and ^{238}U (Figures S4, S5). A weighted average based on the natural abundance of isotopes was calculated for Ca and Mg and used in analyses.

Material properties

The carapace spine and rostral horn tip were tested for hardness and stiffness using a nanoindentation materials testing machine (Nano Hardness Tester, Nanovea, Irvine, CA, USA) equipped with a Berkovich tip. Fresh samples (<12 hours, except for two samples tested within 24 hours) were kept hydrated in seawater until testing. Samples were secured to an aluminum block with cyanoacrylate glue such that the outer surface was facing up. Indentations were performed by applying a load of 40 mN to the outer surface of the sample at loading and unloading rates of 80 mN/min with a 30 sec hold for creep. At least three indents were taken and averaged per sample.

Antenna stiffness

One antenna was removed from each lobster at the base (first segment above the antennae knuckle). The proximal 5 mm of the antennal base was embedded in epoxy (EpoxiCure, Buehler, Lake Bluff, IL, USA) and allowed to cure overnight. Antennae were covered with seawater-soaked paper towels to remain hydrated until testing. The embedded ends of the antennae were clamped in a universal materials testing machine (E1000, 250N load cell, Instron, Norwood, MA, USA) such that the antennae extended laterally. A force was applied at a rate of 20 mm/min to two locations on the antennae, one at 1/3 of the total antenna length ("proximal") and one at 2/3 of the total antenna length ("distal"), until a displacement of 10% of antenna length was reached. The stiffer proximal region of the antenna has a thicker ovular cross section than the distal location, and it lies directly over the carapace when the lobster raises its antennae in a defensive position, so it is believed to be the primary location where force is applied by predators (Lowder, pers. obs.). The tapering of the antennae imbues more flexibility towards the distal end, perhaps to avoid breakage. Flexural stiffness, *EI*, was calculated as:

$$EI = \frac{F_{max} \times antennal\,length^3}{3 \times deflection_{max} \times 0.001}$$

Statistics

All analyses were carried out in R version 3.5.1 (R Core Team, 2019) and associated packages (Wickham, 2016a, 2016b, 2017). We tested survival, growth, cuticle measurements (elemental composition, thickness, material properties), and antennae flexural stiffness data for normality and homogeneity of variances with the Shapiro-Wilk and Bartlett's tests (after the removal of outliers, see below). If data met these conditions, we compared metrics across treatments using one-way ANOVAs and followed with Tukey's Honest Significant Difference test if appropriate. Otherwise, the Kruskal-Wallis with Dunn's test or Welch's corrected ANOVA with Games-Howell *post-hoc* test was used for instances of non-normality and heteroscedasticity, respectively. Carapace length ANOVA residuals were checked for test assumptions visually and with the Shapiro-Wilks test, then log-transformed to meet assumptions. $\alpha = 0.05$ with the exception of elemental data, where we used a Bonferroni correction for repeated measures.

Some cuticle samples had one or two material properties tests that resulted in unusually high values for crustacean cuticle. In many of these instances, the indent was misshapen (stretched in one direction), indicating that the force was not applied perpendicularly to the surface in the manner that is required for accurate measurements. As such, material property outliers of each treatment were calculated and removed *via* the Tukey "fence" or "boxplot rules" method of Q_3 + 1.5 x IQR, where Q_3 is the third quartile and IQR is the interquartile range from the first to the third quartile (Tukey, 1977). The lower "fence" was also calculated, but was always below zero. This method identified outliers ≥ 13.4 GPA in stiffness for the horn and ≥13.1 GPa for the carapace spine. Hardness outliers were ≥ 0.49 GPa for the horn and ≥ 0.52 GPa for the carapace spine.

Results

Survival and molting

All lobsters survived the experimental period and appeared healthy at its conclusion. Molting only occurred in nine out of the sixty-four animals (n=4 in ambient/stable; n=1 in reduced/stable pH; n=3 in reduced/low fluctuating; n=1 in reduced/high fluctuating treatment) and were not included in subsequent analyses. Growth results are included in the supplementary material. The remaining lobsters were molt-staged based on exoskeleton hardness and evidence of apolysis (Travis, 1954; Lyle and MacDonald, 1983) and were determined to be in intermolt, excluding two lobsters that showed signs of apolysis (one from

10.3389/fmars.2022.909017

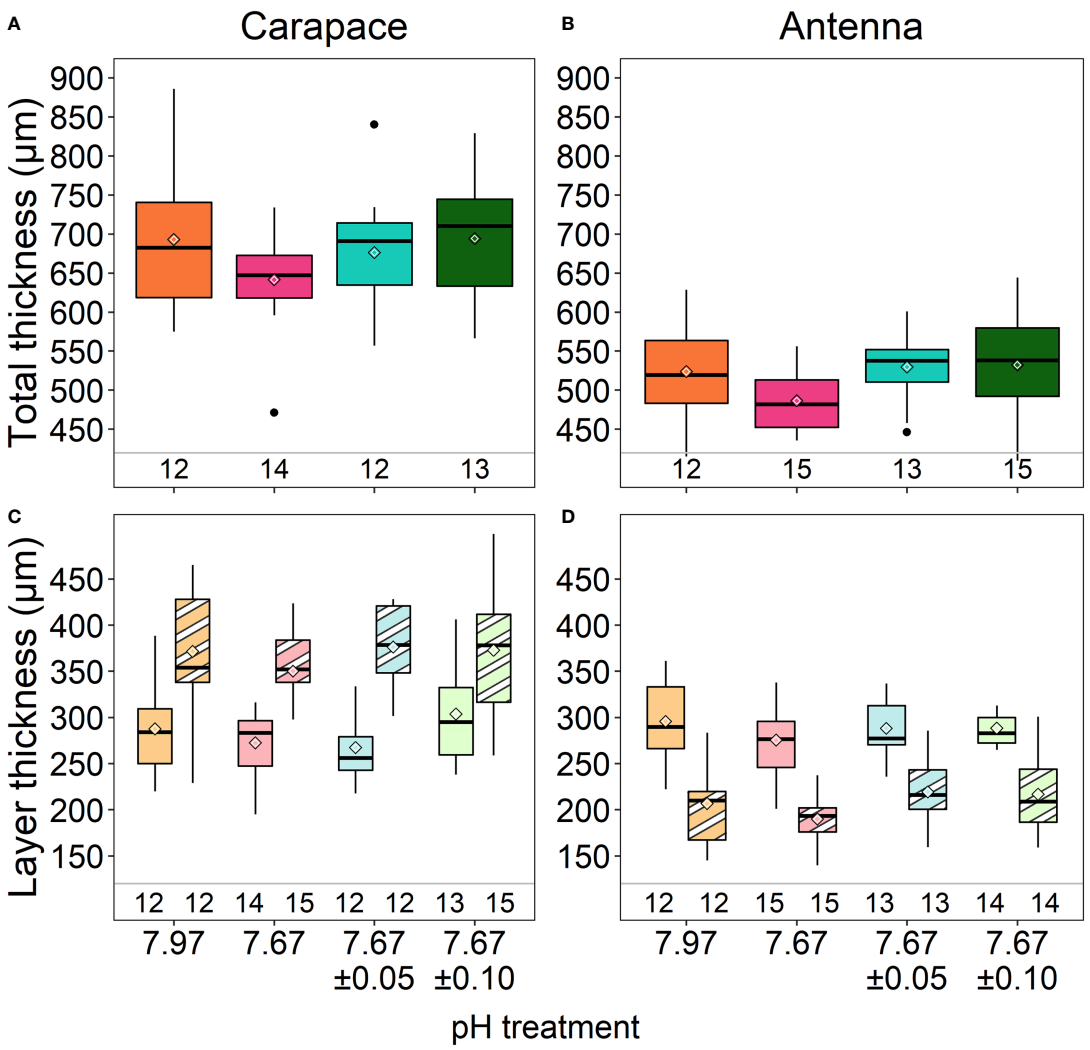

FIGURE 2
Total cuticle thickness of the carapace **(A)** and antennae **(B)** and cuticle layer thickness of the carapace **(C)** and antennae **(D)**. Exocuticle layers are right boxes of each treatment (stripes in **C, D**) and endocuticle layers are left boxes of each treatment (solids in C, D). There were no differences in total thickness or layer thickness of the carapace or antennae among treatments. Box boundaries are the first and third quartiles, whiskers are 1.5 times the interquartile range, the center line is the median, black and white diamonds are the mean, and outliers are solid dots. Values on the bottom of panels denote sample size.

the reduced/stable pH treatment and one from the reduced/high fluctuating pH treatment).

Cuticle structure

There were no significant differences in total cuticle thickness of the carapace (ANOVA: $F_{3,47} = 1.283$, p=0.291) and antennae (ANOVA: $F_{3,51} = 2.006$, p=0.125) among treatments (Figures 2A, B; Table 2; Lowder et al., 2022). Additionally, there were no significant differences in thickness of either the exocuticle or endocuticle layers of either structure (Figures 2C, D; ANOVA, carapace exocuticle: $F_{3,50} = 0.522$, p=0.669; endocuticle: $F_{3,47} = 1.874$, p=0.147; antenna exocuticle: ANOVA: $F_{3,50} = 1.675$, p=0.184; endocuticle: ANOVA: $F_{3,50} = 0.562$, p=0.642).

Cuticle elemental composition

Elemental data from the XL30 SFEG EDX were inconsistent with that of the other EDX instrument and with previous data on lobster cuticle (Lowder, 2019), and were thus excluded from analysis. Analyses carried out with the full set of data did not result in different conclusions. The remaining data (n=5-9 samples per treatment) revealed no significant differences in % wt Ca in either of the carapace layers (Figure 3A; exocuticle: Kruskal-Wallis,

TABLE 2 Mineralization (μmol/mg from ICP-MS measurements; % wt from EDX measurements), ultrastructure (μm from SEM measurements), and mechanical properties (GPa from nanoindentation tests) for the four studied structures across treatments.

Measurement	Structure	Treatment			
		Ambient/stable	Reduced/stable	Reduced/low fluctuating	Reduced/ high fluctuating
Thickness (μm)					
Total cuticle	Abdominal segment	–	–	–	–
	Antenna	524 ± 68	487 ± 40	530 ± 46	532 ± 71
	Carapace	693 ± 92	641 ± 64	676 ± 78	694± 85
	Horn	–	–	–	–
Exocuticle	Abdominal segment	–	–	–	–
	Antenna	207 ± 52	190 ± 26	219 ± 36	217 ± 41
	Carapace	372 ± 67	350 ± 63	376 ± 46	373± 68
	Horn	–	–	–	–
Endocuticle	Abdominal segment	–	–	–	–
	Antenna	296 ± 47	275 ± 40	288 ± 29	288 ± 48
	Carapace	288 ± 50	272 ± 35	267 ± 40	304 ± 47
	Horn	–	–	–	–
Ca					
Total cuticle (μmol/mg)	Abdominal segment	4.65 ± 0.13	4.57 ± 0.18	4.48 ± 0.1	4.59 ± 0.21
	Antenna	–	–	–	–
	Carapace	6.04 ± 0.36	5.95 ± 0.39	5.78 ± 0.31	**5.62 ± 0.25**
	Horn	–	–	–	–
Exocuticle/	Abdominal segment	–	–	–	–
outer ring (% wt)	Antenna	19.3 ± 5.9	15.3 ± 8.4	20.1 ± 10.1	22.7 ± 6.5
	Carapace	20.6 ± 10.5	25.1 ± 6.4	21.6 ± 8.8	20.6 ± 5.1
	Horn	1.3 ± 1.6	0.6 ± 0.2	0.7 ± 0.5	2.6 ± 5.5
Endocuticle/	Abdominal segment	–	–	–	–
core (% wt)	Antenna	27 ± 9.4	21.4 ± 6.3	25.3 ± 11.9	28.2 ± 11
	Carapace	25.2 ± 7.2	30.4 ± 10.9	23 ± 5.3	25.5 ± 6.9
	Horn	18.1 ± 5.8	17.3 ± 5.8	17.9 ± 4.1	17.1 ± 7.6
Mg					
Total cuticle (μmol/mg)	Abdominal segment	0.44 ± 0.02	0.42 ± 0.03	0.44 ± 0.03	0.42 ± 0.03
	Antenna	–	–	–	–
	Carapace	0.47 ± 0.04	0.44 ± 0.04	**0.43 ± 0.04**	**0.41 ± 0.02**
	Horn	–	–	–	–
Exocuticle/	Abdominal segment	–	–	–	–
outer ring (% wt)	Antenna	1.4 ± 0.3	1.1 ± 0.3	1.4 ± 0.1	1.4 ± 0.3
	Carapace	1.6 ± 0.1	1.8 ± 0.3	1.7 ± 0.2	1.7 ± 0.3
	Horn	0.3 ± 0.1	0.2 ± 0.0	0.3 ± 0.2	0.5 ± 0.5
Endocuticle/	Abdominal segment	–	–	–	–
core (% wt)	Antenna	1.1 ± 0.4	1.1 ± 0.2	1.2 ± 0.2	1.2 ± 0.3
	Carapace	1.5 ± 0.2	1.5 ± 0.3	1.6 ± 0.1	1.6 ± 0.3
	Horn	1.1 ± 0.2	1 ± 0.2	1 ± 0.2	0.9 ± 0.4
Material properties					
Stiffness (GPa)	Carapace	15.3 ± 5.3	14.6 ± 5.8	11.9 ± 5.4	11.5 ± 4.1
	Horn	7.0 ± 1.9	7.3 ± 1.9	6.9 ± 2.4	7.2 ± 2
Hardness (GPa)	Carapace	0.32 ± 0.12	0.34 ± 0.13	0.22 ± 0.12	0.24 ± 0.09
	Horn	0.34 ± 0.05	0.36 ± 0.05	0.28 ± 0.03	**0.28 ± 0.05**

Values are mean ± s.d. Bold values are significantly different from values of lobsters in ambient conditions.

χ^2 = 2.154, df=3, p = 0.541; endocuticle: ANOVA, $F_{3,25}$ = 1.081, p = 0.375), horn layers (Figure 3C; outer ring: Kruskal-Wallis, χ^2 = 0.453, df=3, p = 0.929; core: ANOVA, $F_{3,21}$ = 0.04, p = 0.989), and antenna layers (Figure 3B; exocuticle: ANOVA, $F_{3,25}$ = 1.873, p = 0.160; endocuticle: ANOVA, $F_{3,25}$ = 0.658, p = 0.585; Table 2).

There were also no significant differences in % wt Mg in either of the carapace layers (Figure 3D; exocuticle: Welch's ANOVA, $F_{3,11.80}$ = 2.389, p = 0.121; endocuticle: Kruskal-Wallis, χ^2 = 1.266, df=3, p = 0.737), horn layers (Figure 3F); outer ring: Kruskal-Wallis, χ^2 = 0.754, df=3, p = 0.861; core: Kruskal-Wallis, χ^2 = 2.559, df=3, p = 0.465), and antenna layers (Figure 3E; exocuticle: Kruskal-Wallis, χ^2 = 6.061, df=3, p = 0.109; endocuticle: Kruskal-Wallis, χ^2 = 0.968, df=3, p = 0.809; Table 2).

Elemental analysis of the carapace using ICP-MS contrasted with the results obtained from the EDX analysis; the former measured elements over whole volume cuticle whereas the latter measured elements over a surface area whose features can influence electron scattering and thus element quantification. There were significant differences in calcium and magnesium content in the carapace across treatments (calcium: ANOVA,

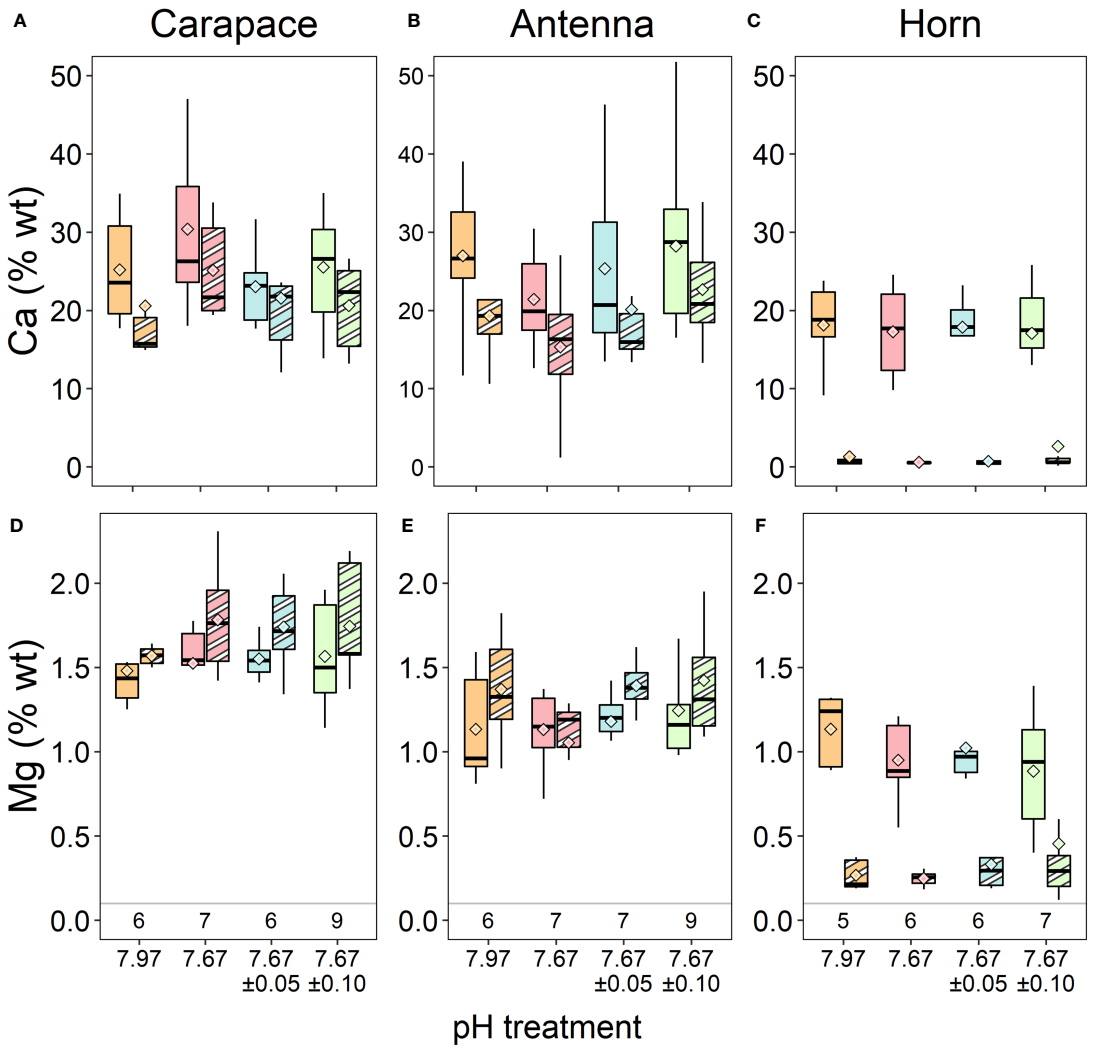

FIGURE 3
Calcium and **(A-C)** Mg **(D-F)** % wt of three exoskeletal structures from EDX measurements. There were no significant differences in either element across treatment conditions. Each structure's exocuticle, or the outer layer in the case of the horn, is represented as the right boxes of each treatment (striped shades), and the endocuticle layers or core of the horn are the left boxes of each treatment (solid shades). Box boundaries are the first and third quartiles, whiskers are 1.5 times the interquartile range, the center line is the median, and black and white diamonds are the mean. Values on the bottom of panels **(D-F)** denote sample size for each structure.

$F_{3,51}$ = 4.313, p = 0.009; magnesium: Kruskal-Wallis, χ^2 = 15.184, df=3, p = 0.002; Figures 4A, C; Table 2). Calcium was 6% lower in the reduced/high fluctuating treatment than the reduced/stable treatment (Tukey HSD, p = 0.043) and 7% lower than the ambient/stable conditions (Tukey HSD, p = 0.010).

Carapace magnesium was significantly lower, by 13%, in the reduced/high fluctuating treatment in comparison to both ambient/stable and the reduced/stable treatments (Tukey HSD, $p \leq 0.006$; Figure 4C; Table 2). The reduced/low fluctuating treatment was also significantly decreased by 8% compared to the ambient/stable treatment (Dunn's test, p = 0.011). Magnesium tended to be lower in the reduced/stable treatment than in ambient/stable (Dunn's test, p = 0.047), and the two fluctuating treatments showed slightly different concentrations (Dunn's test, p = 0.042), although these trends were not statistically significant, as the Bonferroni correction for repeated measures was applied.

In the abdominal segment, there were no significant differences in the calcium (ANOVA: $F_{3,51}$ = 2.21, p=0.098; Figure 4B), and magnesium (ANOVA: $F_{3,51}$ = 1.36, p=0.266; Figure 4D) concentrations between treatments (Table 2).

Cuticle material properties

The carapace spine and rostral horn responded differently to treatment conditions. The carapace spine did not show a significant difference in hardness (ANOVA: $F_{3,37}$ = 2.708, p=0.06; Figure 5A), although the carapaces that were exposed to reduced

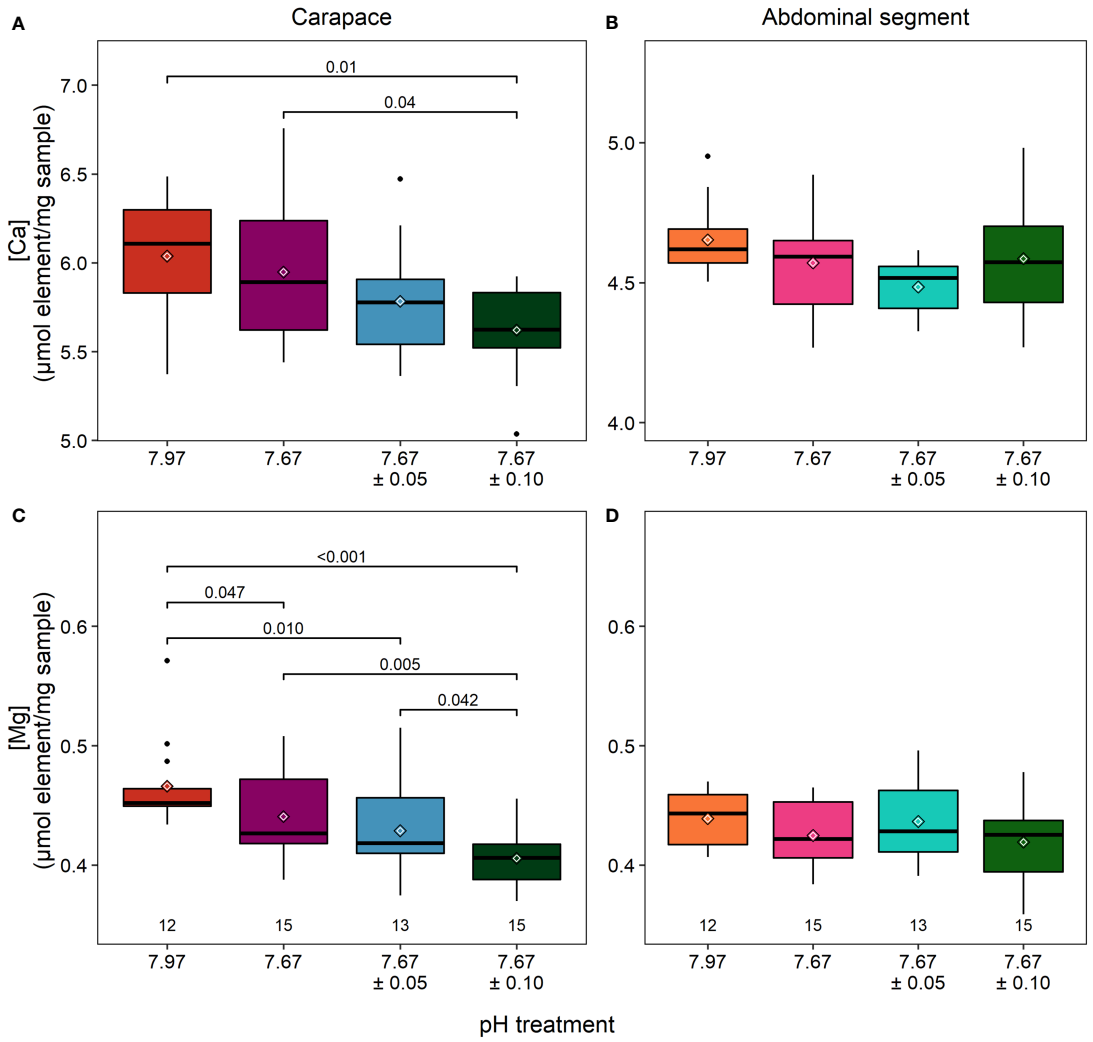

FIGURE 4
Calcium **(A, B)** and magnesium **(C, D)** concentrations measured with ICP-MS. In the carapace of lobsters in the reduced/high fluctuating treatment (7.67 ± 0.10), there was significantly less calcium **(A)** present than in lobsters in ambient/stable conditions. Lobsters in both fluctuating treatments had significantly less magnesium than those in ambient/stable treatments. There were no differences found in the cuticle of the abdominal segment, which had lower and less variable amounts of calcium but similar amounts of Mg to the carapace. Note different axes for panels **(A, B)** α=0.025 after a Bonferroni correction. Box boundaries are the first and third quartiles, whiskers are 1.5 times the interquartile range, the center line is the median, black and white diamonds are the mean, and outliers are solid dots. Values on the bottom of panels denote sample size.

fluctuating pH treatments tended to show lower hardness than those in stable pH treatment, averaging 28% lower. Stiffness was not significantly different across treatments (ANOVA: $F_{3,37}$ = 1.376, p =0.27; Figure 5C; Table 2).

The horns differed significantly in hardness among treatments (ANOVA: $F_{3,36}$ = 7.307, p<0.001) (Figure 5B; Table 2). Horns from lobsters exposed to the two stable pH treatments were statistically the same. However, horn samples from the reduced/high fluctuating treatment were significantly less hard than those from either of the stable pH treatments by 15 - 22% ($p \leq 0.045$). The reduced/low fluctuating treatment horns were lower, but not significantly different, from those in the ambient/stable pH treatment (p=0.050), although they were significantly lower than those in reduced/stable pH treatment (p=0.004). There were no significant differences in horn stiffness among the treatments (ANOVA: $F_{3,36}$ = 0.077, p=0.972; Figure 5D; Table 2).

Antenna stiffness

Mean antennal flexural stiffness (*EI*) at the more flexible distal location did not differ among lobsters in any treatments (Kruskal-Wallis rank sum test, χ^2 = 3.52, df=3, p=0.318) (ambient/stable: 0.004 ± 0.002 Nm^2; reduced/stable: 0.003 ± 0.002 Nm^2; reduced/low fluctuating: 0.003 ± 0.001 Nm^2; reduced/high fluctuating: 0.004 ± 0.002 Nm^2) (Figure 6). At the stiffer proximal location, *EI* was significantly lower in lobsters exposed to reduced/stable pH

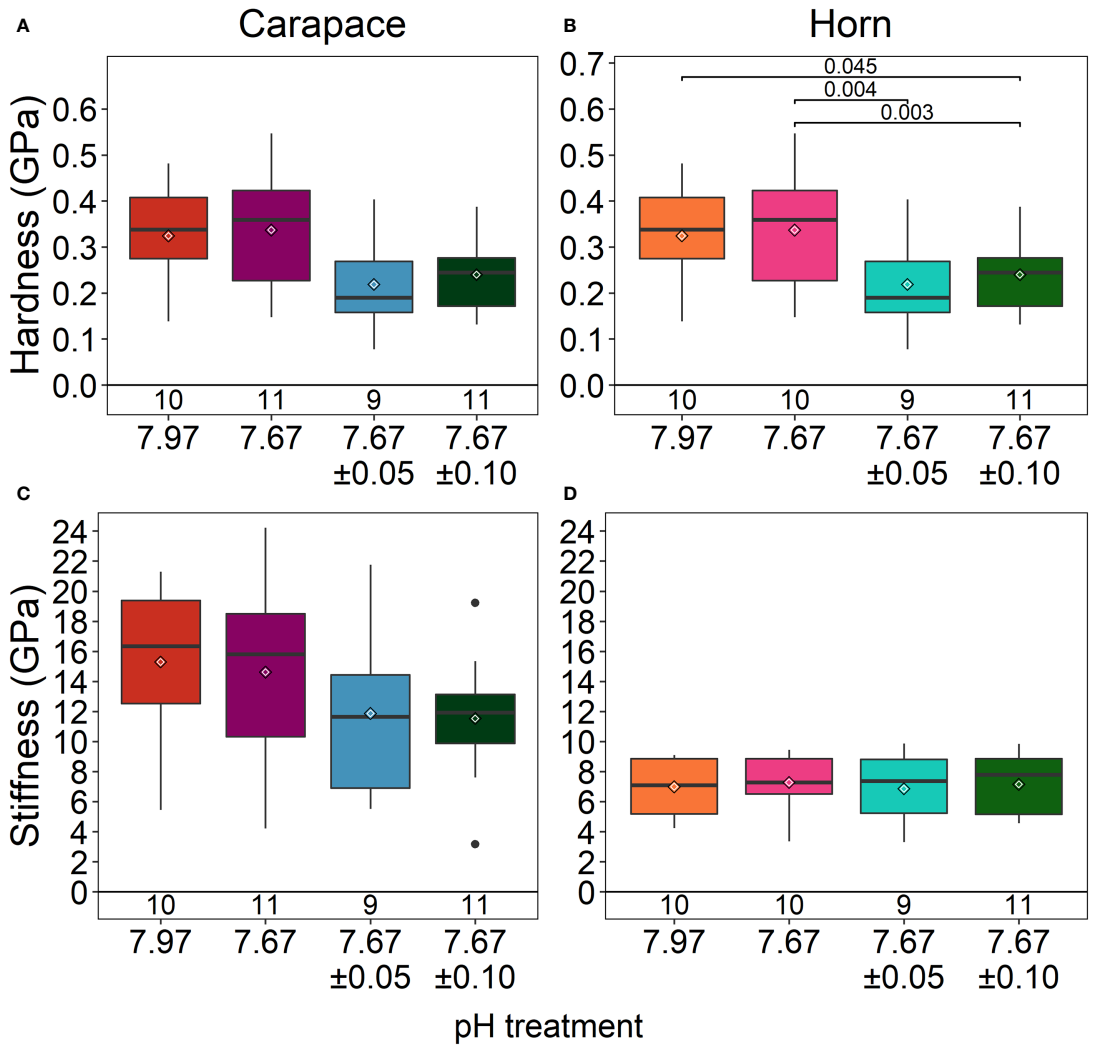

FIGURE 5
Material properties of the carapace spine **(A, C)** and rostral horn **(B, D)**. The carapace spine did not show any differences in material properties among treatments. The horn significantly differed in hardness. Lobsters exposed to reduced/high fluctuating pH conditions had horns that were less hard than those exposed to stable pH conditions (both ambient and reduced pH). Box boundaries are the first and third quartiles, whiskers are 1.5 times the interquartile range, the center line is the median, black and white diamonds are the mean, and outliers are solid dots. Values on the bottom of panels denote sample size.

treatments than lobsters exposed to reduced/high fluctuating pH (Welch's ANOVA: $F_{3,22.55} = 3.15$, p=0.045; Games-Howell posthoc p=0.035). There were no significant differences among the other treatments ($p \geq 0.20$), although *EI* was slightly lower in antennae from the reduced/stable and reduced/low fluctuating treatment than those in ambient conditions (ambient/stable: 0.023 ± 0.012 Nm^2; reduced/stable: 0.018 ± 0.004 Nm^2; reduced/low fluctuating: 0.020 ± 0.004 Nm^2; reduced/high fluctuating: 0.026 ± 0.010 Nm^2).

Discussion

Predation is thought to be the largest source of mortality for juvenile California spiny lobster, *P. interruptus*, until they reach a size refuge against most predators at four to five years of age (Engle, 1979). Mortality rates during this critical life stage could be exacerbated if anti-predation strategies and defenses are compromised by changing ocean carbonate chemistry. OA-like conditions are known to affect the composition of calcified materials (Chan and Connolly, 2013; Kroeker et al., 2013; Davis et al., 2021), potentially disrupting the mechanical properties, though this link is not often studied in crustaceans (Taylor et al., 2015). Furthermore, mineralization effects are generally measured on one or two crustacean body regions, typically the carapace and chelae (Dutil et al., 2000; Boßelmann et al., 2007; Amato et al., 2008), but the strong localization of mineralization and specialization of different structures can lead to differential responses to OA. Lastly, exposure to stable reduced pH experimental conditions does not adequately assess the vulnerability of animals

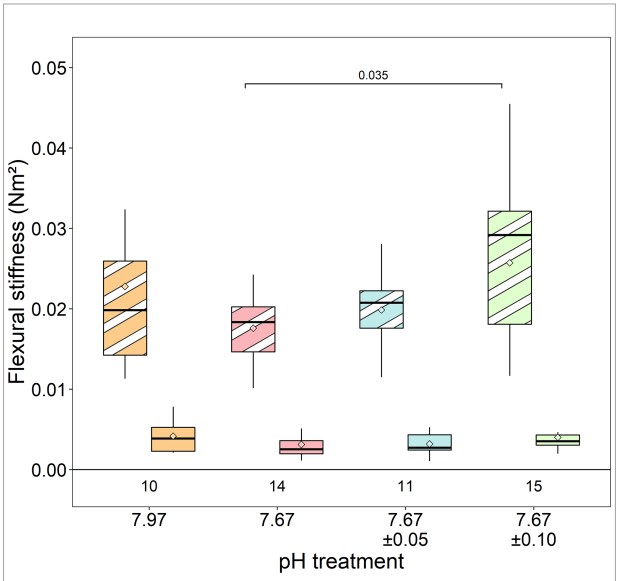

FIGURE 6
Flexural stiffness of the antennae at proximal (striped shades) and distal (solid shades) locations. The low stiffness at the distal location was similar across all treatments. While antennae from the reduced/high fluctuating treatment were stiffer at the proximal base than lobsters in the reduced/stable pH treatment, there were no significant differences in flexural stiffness from the ambient/stable treatment. Box boundaries are the first and third quartiles, whiskers are 1.5 times the interquartile range, the center line is the median, and black and white diamonds are the mean. Values on the bottom of panels denote sample size.

that live in dynamic pH environments (Wahl et al., 2015). Here, we tested the hypotheses that reduced stable pH conditions would affect the mineralization and mechanical properties of exoskeletal defense structures, that the effects would differ in magnitude across structures, and that fluctuating reduced pH conditions would mitigate these effects. After exposing juvenile *P. interruptus* to diurnal conditions that mimic their natural environment under near-future seasonal upwelling and/or OA, we found that most exoskeletal properties were unaffected by the treatment conditions, but that the integrity of some important exoskeletal defenses were compromised in variable ways and not as hypothesized. In particular, changes in mineralization or material properties were observed across key defensive structures (i.e., carapace, rostral horns, and antennae) in ways that were site specific, but absent of typical mineral-mechanical properties relationships. These effects were induced primarily by fluctuating reduced pH conditions and, to a limited extent, stable reduced pH conditions.

Exoskeletal defense integrity

Rostral horns

Spiny lobster rostral horns must be sufficiently hard and stiff to anchor animals in their dens when predators attempt to expel them. The spine-like shape of the horns is effective at locking into the interstices of hard substrate, while high hardness and stiffness limit deformation and yield stress. Structurally, rostral horns differ from the typical cuticle template by having only two layers, an outer and inner core (Lowder, 2019). The outer layer of the horn is poorly mineralized in comparison to typical crustacean cuticle, with just 1.4% Ca and 0.3% Mg. Neither Ca or Mg percentages were affected by reduced pH conditions in either layer, but hardness of the horn tips was lower in the reduced pH fluctuating conditions (both low and high fluctuating). The magnitude of this change in hardness is slight (<0.1 GPa, or 15%) compared to the decrease in microhardness observed in the chelae of juvenile blue and red king crabs (~44 VHN, or 46%) (Coffey et al., 2017). While red king crabs exhibited this decrease after exposure to pH 7.8, blue king crabs did so under a more extreme pH of 7.5; however, both species were exposed for a longer period of time (1 year) during which these effects manifested. It is unknown if the magnitude of change observed in spiny lobsters after three months of exposure would result in notable effects on lobster anchoring ability, but it is possible that longer exposure encompassing exoskeleton regeneration through one or more molt cycles could result in more dramatic effects.

We could not separate the horn layers for analysis of Ca and Mg content using the ICP-MS method, though EDX is sufficient for documenting differences in elemental composition (Fabritius et al., 2012; Taylor et al., 2015). The rostral horns have high amounts of halogens, such as chlorine, in the outer ring (Lowder, 2019), similar to the dactyl tips of crabs that scrape algae from rocks (Cribb et al., 2009). The replacement of calcium carbonate with halogenated compounds provides structures with greater toughness rather than hardness, which is beneficial for avoiding wear and breakage on rocky surfaces (Cribb et al., 2009; Schofield et al., 2009). This would be functionally important for the rostral horns that must lodge into the rocky underhangs of their shelter. It is interesting though that horn hardness was affected by reduced, fluctuating pH conditions despite its uncalcified state, hinting at a potentially complex interplay of elements under different ocean carbon chemistry parameters.

Antenna

Lobsters use their antennae as cantilevers to push away animals and maintain their distance (Kanciruk, 1980; Spanier and Zimmer-Faust, 1988). Sufficient flexural stiffness of the antennae is necessary to produce and maintain forces that hold predators at bay. In general, antennal cuticle has a thinner exocuticle layer compared to carapace cuticle, but both have similar Ca and Mg content. Flexural stiffness of the antenna is derived by the greater second moment of area associated with its hollow, tubular design, but it is also dependent on cuticle thickness and stiffness. Neither cuticle thickness nor mineral content of the antennae were affected by reduced pH conditions, unlike the carapace. Though there were no detectable changes in structure and composition, stiffness at the proximal base of the antennae in reduced/stable pH conditions was significantly reduced, by 31%, relative to

the reduced pH/high fluctuating conditions. The mechanism underlying this change in bending stiffness is unclear, but may stem from weakened articulations between antennal annuli. Antennae breakage tends to occur in these regions (Lowder, pers. obs.), which warrants detailed morphological analysis.

Carapace

Should lobsters fail to keep predators at bay, their last line of exoskeletal defense is their armored carapace. The spiny lobster carapace is covered with thick, flattened spines and is more heavily mineralized than the abdominal segments (Lowder, 2019). These attributes enhance hardness and stiffness, consequently providing greater resistance to the piercing and crushing forces of predator attacks, such as by the California sheephead. The abdomen, in contrast, facilitates the tail flip escape response and is not exposed to predators when the animal is sheltering. While there was no change to material properties after medium-term exposure to reduced pH/fluctuating conditions, carapace mineralization (both Ca and Mg) decreased and there was no change within the abdominal segment. The higher concentration of mineral as calcium carbonate and magnesian calcite in the carapace may have made it more favorable to draw from for potential hemolymph buffering under reduced pH conditions (Henry et al., 1981; Spicer et al., 2007). Thus, structures with greater mineral availability, and which benefit the most from the hardness that mineralization provides, may be more vulnerable to losing it in reduced pH/high pCO_2 conditions.

Discrepancies between elemental composition measured with ICP-MS and EDX are likely due to differences in the sensitivities of the techniques and/or in the cuticle regions sampled. Here, ICP-MS analysis revealed decreases to mineralization in reduced pH/fluctuating conditions, whereas no decrease was identified by EDX. Measuring elements over a 2-dimensional surface with EDX, compared to a volume of material with ICP-MS, captures more variation within and between cuticle samples, introducing greater variability, as observed in our data. EDX is also sensitive to surface morphology and sample preparation, which affects electron scattering and element detection. Furthermore, using EDX we only measured elements across regions of the endo- and exo-cuticle layers, whereas with ICP-MS we measured all layers, including the epicuticle. The distribution of mineral across cuticle layers in spiny lobsters is not well-documented, but the American lobster cuticle exhibits a defined calcitic layer near the outermost region of the exocuticle, bordering the epicuticle (Al-Sawalmih et al., 2008; Kunkel, 2013). If spiny lobster cuticles are similar, then changes to the mineralization of this layer would more likely be detected through our ICP-MS measurements of the whole cuticle, rather than our EDX sampling that did not capture this particular region.

Tangled links between composition and properties

Among mineralized organisms, changes to Ca and Mg content after exposure to reduced pH are assumed to belie changes to the mechanical function of calcified structures, but the limited studies testing this link so far defy expectations. In one study, increases in Mg content in the raptorial appendage of mantis shrimp exposed to ocean acidification-like conditions did not result in significant changes to the hardness or stiffness of the cuticle (deVries et al., 2016). In another study, Ca content increased in the carapace and chela of blue king crabs and red king crabs, respectively, but only the chela mechanical properties in both species changed (Coffey et al., 2017). For tanner crabs, an increase in carapace Mg and decrease in Ca did not result in any changes to microhardness, but chelae without significant alterations in mineralization experienced reductions in microhardness (Dickinson et al., 2021). In the present study, both Ca and Mg content decreased in the carapace of California spiny lobsters, but there was no significant change in cuticle hardness or stiffness. In all of these studies of crustaceans, changes in mineral content were less than 20%, which may not be of sufficient magnitude to induce measurable changes in nanomechanical properties. Several studies have established coarse correlations between the degree of mineralization and mechanical properties in crustacean cuticle (Currey at al., 1982; Raabe et al., 2005; Taylor and Kier 2006; Sachs et al., 2006; Fabritius et al., 2012; Weaver et al., 2012; Rosen et al., 2020), but its complex structure and variation among species make it difficult to parse out fine-scale relationships and potential thresholds.

In contrast, cuticle mechanical properties may change independently from adjustments to mineral content, as observed here in the rostral horns of the spiny lobster that decreased in hardness without any corresponding changes to mineral content. Both cuticle structure (i.e., total thickness, layer thickness and stacking density) and mineral phase contribute to cuticle mechanical properties (Raabe et al., 2005). Changes to the former have not been observed in most crustaceans exposed to reduced pH conditions (Taylor et al., 2015; deVries et al., 2016; Lowder et al., 2017; Coffey et al., 2017), including species whose mechanical integrity was compromised (Coffey et al., 2017). Structural level changes, thus, are unlikely to be the mechanism driving observable effects in mechanical properties. The present study, as well as other crustacean OA studies, implicitly assume that the protein-chitin matrix of the cuticle remains unchanged, so that changes to the mineral:matrix ratios governing stiffness are driven by mineral content alone. What has yet to be widely observed in OA research are potential changes to the mineral phase in crustaceans. Crustaceans can manipulate calcium carbonate forms and use amorphous calcium carbonate, magnesian calcite, and calcite (Huner et al., 1979; Vigh and Dendinger, 1982; Addadi

et al., 2003; Dillaman et al., 2005; Boßelmann et al., 2007), which may allow species to compensate for mineralization changes due to OA while maintaining structural function. Indeed, Tanner crabs that were post terminal molt appeared to shift amorphous calcium carbonate to calcite after two years of exposure to reduced pH conditions (Dickinson et al., 2021).

Crustacean cuticle is built with multiple levels of hierarchical structure (Raabe et al., 2005) that adds complexity to the large-scale link between structure, composition, and mechanical function under OA-like conditions. This link becomes clouded in other marine calcifiers as well, including mussels that develop more brittle and less stiff shell regions without any direct change in structure or composition (Fitzer et al., 2015). Consequently, direct relationships between compositional changes under OA-like conditions and material properties have not been consistently identified, and the perceived implications of observed changes to mineralization should be tested when possible.

Reduced pH affects intermolt exoskeleton

The effects of OA-like conditions on crustacean mineralization should be maximally expressed during molting, when animals shed and rapidly build a new exoskeleton. Mineral deposition peaks during the early postmolt period, but is otherwise considered stable throughout the duration of intermolt, except when mineral is potentially drawn away to be stored in gastroliths prior to the next molt (Shechter et al., 2008). As only two individuals (one from the reduced/stable pH treatment and one from the reduced/high fluctuating pH treatment) showed indications of entering the premolt stage (softened exoskeleton and apolysis) at the conclusion of the experiment, variations in molt stage do not likely explain variation in measurements. Juvenile California spiny lobsters of the size used in this study molt annually (California Department of Fish and Wildlife, 2004), and only a few lobsters from each treatment molted over the three month duration of this experiment. Yet, significant changes in mineralization and material properties occurred in the absence of molting, which has also been observed in Tanner crabs past their terminal molt (Dickinson et al., 2021). We found significant decreases in both Ca and Mg in the carapace, hardness in the rostral horns, and flexural stiffness in the antennae of intermolt lobsters, demonstrating that the fully-formed exoskeleton of intermolt animals is sensitive to reduced pH conditions.

Crustaceans use bicarbonate to regulate internal acid-base chemistry under external high pCO_2 conditions and the carbonate minerals in the cuticle can be one source of the ion (Henry et al., 1981). A significant decrease in calcium concentration in the carapace was only found in the reduced/high fluctuating treatment, potentially indicating that the lowest pH values of the experiment reached in that treatment at night (7.57) may have triggered calcium carbonate dissolution from the carapace to use for buffering. Magnesium concentration showed significant decreases from ambient conditions in all three reduced pH treatments. Magnesium is likely in the form of magnesian calcite, a more soluble form of calcite, and may have been drawn out first (Davis et al., 2000).

In other juvenile crustaceans, mineralization is often not affected by exposure to pH conditions expected within the next century. For example, there was no change in either [Mg] or [Ca] at moderate (0.25 pH unit) decreases in pH for the early juvenile stage of the American lobster, *H. americanus*, after five weeks of exposure (Menu-Courey et al., 2018). Juvenile blue swimming crabs and hermit crabs exposed to reduced pH conditions incurred no changes in Ca content, but hermit crabs exhibited small increases in Mg (Glandon et al., 2018; Ragagnin et al., 2018). The above results were all found in animals that had molted during the experiment. In *Homarus gammarus* that didn't molt, there was no change in Mg and Ca after five weeks of exposure to a 0.4 unit decrease in pH (Small et al., 2016), although longer-term exposure might induce detectable changes.

Fluctuating pH conditions may exacerbate effects of reduced pH

Our results indicate that future scenarios of fluctuating pH conditions are not beneficial to *P. interruptus*, despite the current natural fluctuations they experience in kelp forests on diurnal and seasonal scales (Frieder et al., 2012; Kapsenberg and Hofmann, 2016; Kekuewa et al., 2020). While each reduced pH treatment had the same mean pH value, fluctuations above this value were hypothesized to provide a short, daily refuge period when processes like calcification can mainly be carried out (Wahl et al., 2018). Indeed, we found distinct differences in exoskeletal defenses between fluctuating and stable reduced pH conditions, but they were contrary to expectations. Mineralization (e.g., carapace Mg concentration) and material properties (e.g., rostral horn hardness) were significantly reduced in fluctuating conditions, but were unaffected by stable pH exposure. At the same time, antennae flexural stiffness was significantly lower in reduced, stable pH conditions.

Like some organisms, juvenile spiny lobsters may find fluctuating low pH conditions stressful; fluctuating reduced pH conditions raised oxidative stress levels in the mussel *Mytilus edulis* (Mangan et al., 2017). In this study, negative effects tended to be greater under reduced pH with high fluctuations than with low fluctuations. Potentially, the negative effects may result from the pH dropping below a threshold value at night around 7.55-7.60 pH units, which lobsters do not appear to encounter frequently, if at all, in the kelp forest habitat where they were collected (Frieder et al., 2012). Thus, OA may breach the sensitivity thresholds of organisms in fluctuating environments more rapidly than in relatively stable habitats, necessitating consideration of dynamics when developing

predictions for when impacts on species and ecosystems will become more apparent.

Conclusions

In this study on juvenile California spiny lobsters, we found that fluctuating reduced pH conditions affect the mineral composition and mechanical properties of some of their exoskeletal defense structures, thereby adding *P. interruptus* to the list of species sensitive to OA-like conditions. This is the first study to establish spiny lobsters' exoskeleton sensitivity to reduced pH, adding to the evidence of sensory impacts to this group (Ross and Behringer, 2019; Gravinese et al., 2020; Boco et al., 2021) that also has implications for predator defenses. The effects were variable across exoskeletal structures, demonstrating localized responses within an individual that should be accounted for when assessing vulnerability across crustacean species. While the magnitudes of these effects were not appreciably large, it is noteworthy that significant changes to the exoskeleton occurred during the intermolt phase, when the cuticle is generally considered to be stable. This observation reveals that the crustacean exoskeleton can be continuously responsive to environmental pH/pCO_2 conditions, and not just during the peak post molt period. Furthermore, the correlation between mineralization and mechanical properties is not always straightforward under OA-like conditions such that changes in mineralization are not necessarily a good indicator of impacts on mechanical properties. Thus, assumptions about mechanical integrity and function cannot be made based on mineral content alone.

Worldwide, 19 *Panulirus* species (Ptacek et al., 2001) live in shallow, dynamic habitats, such as coral reefs, rocky reefs, and kelp forests. Our study on the temperate *P. interruptus* shows that the natural daily fluctuations in pH typical of these habitats does not necessarily afford spiny lobsters with a helpful respite from greater pH variations associated with climate change predictions. Rather, reduced/fluctuating pH conditions induced exoskeletal changes not observed under stable reduced pH. Dynamic pH conditions should therefore be considered when assessing the vulnerabilities of other species of spiny lobsters, as well as other crustaceans occupying these habitats. Under future ocean conditions, the California spiny lobster may engage with predators using altered exoskeletal defenses that could potentially affect the outcomes of these interactions.

Data availability statement

The datasets presented in this study can be found in online repositories. The names of the repository/repositories and accession number(s) can be found below: Data and metadata are available through PANGAEA: Lowder, Kaitlyn; deVries, Maya S; Hattingh, Ruan; Day, James M D; Andersson, Andreas J; Zerofski, Phillip; Taylor, Jennifer (2022): Exoskeletal predator defenses of juvenile California spiny lobsters (*Panulirus interruptus*) are affected by fluctuating ocean acidification. PANGAEA, https://doi.org/10.1594/PANGAEA.945362.The R code is accessible at: https://github.com/kblowder/Spiny-lobster-exoskeleton-OA.

Author contributions

KL and JT conceptualized the research and wrote the manuscript. KL carried out the experimental study, water chemistry measurements, hardness and stiffness nanoindentation measurements, SEM and EDX measurements, statistical analyses, and aided in animal collection. JT carried out flexural stiffness and ICP-MS measurements. MdV helped carry out SEM and EDX measurements, and RH aided in ICP-MS measurement and analysis. JD contributed to ICP-MS analysis. AA aided in designing water chemistry treatments and analyzing water chemistry results. PZ led animal collection and aided in experimental setup. JD, AA, and MdV edited the manuscript. All authors contributed to the article and approved the submitted version.

Funding

This work was partially supported through access and utilization of the NanoEngineering Materials Research Center (NE-MRC) and the Nano3 facility at UC San Diego. This work was supported by the National Science Foundation Graduate Research Fellowship Program, the UC San Diego Frontiers of Innovation Scholars Program, and the PADI Foundation to KL.

Acknowledgments

Many volunteers were critical for carrying out this work: Cierra Kelly, Jack Shurtz, Duc Tran, Steven Ly, Eric Young, Grace Chan, Kyle Perdue, Zoe Sebright, and Alex Hill. Travis Buck, Kevin Hovel, Brett Pickering, Lyndsay Sutterley, Matt Costa, and Georgie Zelanak either provided traps, helped set them up, or helped recover trapped lobsters. Sebastian Davis, Yaamini Venkataraman, and Summer Webb helped collect water samples from La Jolla seagrass beds. David Cervantes from the Dickson Laboratory provided the sampling protocol and analyzed water samples. Scripps Coastal & Open Ocean BiogeochemistrY lab members, including Alyssa Griffin, Sam Kekuewa, and Ariel Pezner, helped train and troubleshoot while analyzing experimental water samples. Sabine Faulhaber provided training at the NanoEngineering Materials

Research Center (NE-MRC). We also thank the editor and reviewers for their thoughtful comments. Portions of this work are contained in the dissertation of KL (Lowder, 2019).

Conflict of interest

The authors declare that the research was conducted in the absence of any commercial or financial relationships that could be construed as a potential conflict of interest.

Publisher's note

All claims expressed in this article are solely those of the authors and do not necessarily represent those of their affiliated organizations, or those of the publisher, the editors and the reviewers. Any product that may be evaluated in this article, or claim that may be made by its manufacturer, is not guaranteed or endorsed by the publisher.

Supplementary material

The Supplementary Material for this article can be found online at: https://www.frontiersin.org/articles/10.3389/fmars.2022.909017/full#supplementary-material

References

Addadi, L., Raz, S. and Weiner, S. (2003). Taking advantage of disorder: amorphous calcium carbonate and its roles in biomineralization. *Advanced Materials* 15, 959–970. doi: 10.1002/adma.200300381

Alenius, B. and Munguia, P. (2012). Effects of pH variability on the intertidal isopod, *Paradella dianae*. *Mar. Freshw. Behav. Physiol.* 45, 245–259. doi: 10.1080/10236244.2012.727235

Al-Sawalmih, A., Li, C., Siegel, S., Fabritius, H., Yi, S., Raabe, D., et al. (2008). Microtexture and chitin/calcite orientation relationship in the mineralized exoskeleton of the American lobster. *Advanced Funct. materials* 18, 3307–3314. doi: 10.1002/adfm.200800520

Amato, C. G., Waugh, D. A., Feldmann, R. M. and Schweitzer, C. E. (2008). Effect of calcification on cuticle density in decapods: a key to lifestyle. *J. Crustacean Biol.* 28, 587–595. doi: 10.1651/08-2985.1

Andersson, A. J., Kline, D. I., Edmunds, P. J., Archer, S. D., Bednaršek, N., Carpenter, R. C., et al. (2015). Understanding ocean acidification impacts on organismal to ecological scales. *Oceanography* 28, 16–27. doi: 10.5670/oceanog.2015.27

Andersson, A. and Mackenzie, F. (2012). Revisiting four scientific debates in ocean acidification research. *Biogeosciences* 9, 893–905. doi: 10.5194/bg-9-893-2012

Auzoux-Bordenave, S., Wessel, N., Badou, A., Martin, S., M'zoudi, S., Avignon, S., et al. (2020). Ocean acidification impacts growth and shell mineralization in juvenile abalone (*Haliotis tuberculata*). *Mar. Biol.* 167, 1–14. doi: 10.1007/s00227-019-3623-0

Avignon, S., Auzoux-Bordenave, S., Martin, S., Dubois, P., Badou, A., Coheleach, M., et al. (2020). An integrated investigation of the effects of ocean acidification on adult abalone (*Haliotis tuberculata*). *ICES J. Mar. Sci.* 77, 757–772. doi: 10.1093/icesjms/fsz257

Barshaw, D. E., Lavalli, K. L. and Spanier, E. (2003). Offense versus defense: responses of three morphological types of lobsters to predation. *Mar. Ecol. Prog. Ser.* 256, 171–182. doi: 10.3354/meps256171

Boßelmann, F., Romano, P., Fabritius, H., Raabek, D. and Epple, M. (2007). The composition of the exoskeleton of two crustacea: The American lobster H*omarus americanus* and the edible crab *Cancer pagurus*. *Thermochimica Acta* 463, 65–68. doi: 10.1016/j.tca.2007.07.018

Boco, S. R., Pitt, K. A. and Melvin, S. D. (2021). Ocean acidification impairs the physiology of symbiotic phyllosoma larvae of the lobster *Thenus australiensis* and their ability to detect cues from jellyfish. *Sci. Total Environ.* 793, 148679. doi: 10.1016/j.scitotenv.2021.148679

Briones-Fourzán, P., Pérez-Ortiz, M. and Lozano-Álvarez, E. (2006). Defense mechanisms and antipredator behavior in two sympatric species of spiny lobsters, *Panulirus argus* and *P. guttatus*. *Mar. Biol.* 149, 227–239. doi: 10.1007/s00227-005-0191-2

California Department of Fish and Wildlife (2004). *Annual status of the fisheries report through 2003* (California Department of Fish and Wildlife). Berkeley, CA, United States

Challener, R. C., Robbins, L. L. and McClintock, J. B. (2015). Variability of the carbonate chemistry in a shallow, seagrass-dominated ecosystem: implications for ocean acidification experiments. *Mar. Freshw. Res.* 67, 163–172. doi: 10.1071/MF14219

Chan, F., Barth, J. A., Blanchette, C. A., Byrne, R. H., Chavez, F., Cheriton, O., et al. (2017). Persistent spatial structuring of coastal ocean acidification in the California current system. *Sci. Rep.* 7, 1–7. doi: 10.1038/s41598-017-02777-y

Chan, N. C. and Connolly, S. R. (2013). Sensitivity of coral calcification to ocean acidification: a meta-analysis. *Global Change Biol.* 19, 282–290. doi: 10.1111/gcb.12011

Chen, P.-Y., Lin, A. Y.-M., McKittrick, J. and Meyers, M. A. (2008). Structure and mechanical properties of crab exoskeletons. *Acta Biomaterialia* 4, 587–596. doi: 10.1016/j.actbio.2007.12.010

Clark, H. R. and Gobler, C. J. (2016). Diurnal fluctuations in CO_2 and dissolved oxygen concentrations do not provide a refuge from hypoxia and acidification for early-life-stage bivalves. *Mar. Ecol. Prog. Ser.* 558, 1–14. doi: 10.3354/meps11852

Coffey, W. D., Nardone, J. A., Yarram, A., Long, W. C., Swiney, K. M., Foy, R. J., et al. (2017). Ocean acidification leads to altered micromechanical properties of the mineralized cuticle in juvenile red and blue king crabs. *J. Exp. Mar. Biol. Ecol.* 495, 1–12. doi: 10.1016/j.jembe.2017.05.011

Cribb, B. W., Rathmell, A., Charters, R., Rasch, R., Huang, H. and Tibbetts, I. R. (2009). Structure, composition and properties of naturally occurring non-calcified crustacean cuticle. *Arthropod Structure Dev.* 38, 173–178. doi: 10.1016/j.asd.2008.11.002

Currey, J. D., Nash, A., and Bonfield, W. (1982). Calcified cuticle in the stomatopod smashing limb. Journal of Materials Science 17, 1939–1944. doi: 10.1007/BF00540410

Currey, J. D. (1984). Effects of differences in mineralization on the mechanical properties of bone. *Philos. Trans. R. Soc. London. B Biol. Sci.* 304, 509–518. doi: 10.1098/rstb.1984.0042

Davis, K. L., Colefax, A. P., Tucker, J. P., Kelaher, B. P. and Santos, I. R. (2021). Global coral reef ecosystems exhibit declining calcification and increasing primary productivity. *Commun. Earth Environ.* 2, 1–10. doi: 10.1038/s43247-021-00168-w

Davis, K. J., Dove, P. M. and De Yoreo, J. J. (2000). The role of Mg^{2+} as an impurity in calcite growth. *Science* 290, 1134–1137. doi: 10.1126/science.290.5494.1134

deVries, M. S., Webb, S. J., Tu, J., Cory, E., Morgan, V., Sah, R. L. et al. (2016). Stress physiology and weapon integrity of intertidal mantis shrimp under future ocean conditions. *Sci. Rep.* 6, 38637. doi: 10.1038/srep38637

Dickinson, G. H., Bejerano, S., Salvador, T., Makdisi, C., Patel, S., Long, W. C., et al. (2021). Ocean acidification alters properties of the exoskeleton in adult tanner crabs, *Chionoecetes bairdi*. *J. Exp. Biol.* 224, jeb232819. doi: 10.1242/jeb.232819

Dickson, A. G. (1990). Standard potential of the reaction: AgCl (s)+ $12H_2$ (g)= Ag (s)+ HCl (aq), and the standard acidity constant of the ion HSO_2^- in synthetic sea water from 273.15 to 318.15 K. *J. Chem. Thermodynamics* 22, 113–127. doi: 10.1016/0021-9614(90)90074-Z

Dickson, A. and Millero, F. J. (1987). A comparison of the equilibrium constants for the dissociation of carbonic acid in seawater media. *Deep Sea Res. Part A. Oceanographic Res. Papers* 34, 1733–1743. doi: 10.1016/0198-0149(87)90021-5

Dickson, A. G., Sabine, C. L. and Christian, J. R. (2007). *Guide to best practices for ocean CO_2 measurements* (Sidney, BC: North Pacific Marine Science Organization).

Dillaman, R., Hequembourg, S. and Gay, M. (2005). Early pattern of calcification in the dorsal carapace of the blue crab, *Callinectes sapidus*. *J. Morphology* 263, 356–374. doi: 10.1002/jmor.10311

Duquette, A., McClintock, J. B., Amsler, C. D., Pérez-Huerta, A., Milazzo, M. and Hall-Spencer, J. M. (2017). Effects of ocean acidification on the shells of four Mediterranean gastropod species near a CO_2 seep. *Mar. pollut. Bull.* 124, 917–928. doi: 10.1016/j.marpolbul.2017.08.007

Dutil, J., Rollet, C., Bouchard, R. and Claxton, W. (2000). Shell strength and carapace size in non-adult and adult male snow crab (*Chionoecetes opilio*). *J. Crustacean Biol.* 20, 399–406. doi: 10.1163/20021975-99990051

Engle, J. M. (1979). *Ecology and growth of juvenile California spiny lobster, panulirus interruptus (Randall)* (Los Angeles, California, United States: University of Southern California).

Fabritius, H.-O., Karsten, E. S., Balasundaram, K., Hild, S., Huemer, K. and Raabe, D. (2012). Correlation of structure, composition and local mechanical properties in the dorsal carapace of the edible crab *Cancer pagurus*. *Z. für Kristallographie-Crystalline Materials* 227, 766–776. doi: 10.1524/zkri.2012.1532

Fitzer, S. C., Zhu, W., Tanner, K. E., Phoenix, V. R., Kamenos, N. A. and Cusack, M. (2015). Ocean acidification alters the material properties of *Mytilus edulis* shells. *J. R. Soc. Interface* 12, 20141227. doi: 10.1098/rsif.2014.1227

Frieder, C. A., Gonzalez, J. P., Bockmon, E. E., Navarro, M. O. and Levin, L. A. (2014). Can variable pH and low oxygen moderate ocean acidification outcomes for mussel larvae? *Global Change Biol.* 20, 754–764. doi: 10.1111/gcb.12485

Frieder, C. A., Nam, S. H., Martz, T. R. and Levin, L. A. (2012). High temporal and spatial variability of dissolved oxygen and pH in a nearshore California kelp forest. *Biogeosciences* 9, 3917–3930. doi: 10.5194/bg-9-3917-2012

Glandon, H. L., Kilbourne, K. H., Schijf, J. and Miller, T. J. (2018). Counteractive effects of increased temperature and pCO_2 on the thickness and chemistry of the carapace of juvenile blue crab, *Callinectes sapidus*, from the Patuxent River, Chesapeake Bay. *J. Exp. Mar. Biol. Ecol.* 498, 39–45. doi: 10.1016/j.jembe.2017.11.005

Gravinese, P. M., Page, H. N., Butler, C. B., Spadaro, A. J., Hewett, C., Considine, M., et al. (2020). Ocean acidification disrupts the orientation of postlarval Caribbean spiny lobsters. *Sci. Rep.* 10, 1–9. doi: 10.1038/s41598-020-75021-9

Henry, R., Kormanik, G., Smatresk, N. and Cameron, J. (1981). The role of $CaCO_2$ dissolution as a source of HCO_3^- for the buffering of hypercapnic acidosis in aquatic and terrestrial decapod crustaceans. *J. Exp. Biol.* 94, 269–274. doi: 10.1242/jeb.94.1.269

Higgins, B. A., Law, C. J. and Mehta, R. S. (2018). Eat whole and less often: ontogenetic shift reveals size specialization on kelp bass by the California moray eel, *Gymnothorax mordax*. *Oecologia*. 188(3), 875-887 doi: 10.1007/s00442-018-4260-x

Hofmann, G. E., Smith, J. S., Johnson, K. S., Uwe, S., Levin, L. A., Fiorenza, M., et al. (2011). High-frequency dynamics of ocean pH: a multi-ecosystem comparison. *PloS One* 6:e28983. doi: 10.1371/journal.pone.0028983

Huner, J. V., Colvin, L. B. and Reid, B. (1979). Whole-body calcium, magnesium and phosphorous levels of the California brown shrimp, *Penaeus californiensis* (Decapoda: Penaeidae) as functions of molt stage. *Comp. Biochem. Physiol. Part A: Physiol.* 64, 33–36. doi: 10.1016/0300-9629(79)90426-2

IPCC (2014). Climate Change 2014: Synthesis Report. Contribution of Working Groups I, II and III to the Fifth Assessment Report of the Intergovernmental Panel on Climate Change [Core Writing Team, Pachauri, R. K. and Meyer, L. A. (eds.)].

James, R. K., van Katwijk, M. M., van Tussenbroek, B. I., van der Heide, T., Dijkstra, H. A., van Westen, R. M., et al. (2019). Water motion and vegetation control the pH dynamics in seagrass-dominated bays. *Limnology Oceanography*. 65(2), 349-362. doi: 10.1002/lno.11303

Jarrold, M. D., Humphrey, C., McCormick, M. I. and Munday, P. L. (2017). Diel CO_2 cycles reduce severity of behavioural abnormalities in coral reef fish under ocean acidification. *Sci. Rep.* 7, 10153. doi: 10.1038/s41598-017-10378-y

Johnson, M. D., Rodriguez, L. M., O'Connor, S. E., Varley, N. F. and Altieri, A. H. (2019). pH variability exacerbates effects of ocean acidification on a Caribbean crustose coralline alga. *Front. Mar. Sci.* 6, 150. doi: 10.3389/fmars.2019.00150

Johnson, Z. I., Wheeler, B. J., Blinebry, S. K., Carlson, C. M., Ward, C. S. and Hunt, D. E. (2013). Dramatic variability of the carbonate system at a temperate coastal ocean site (Beaufort, North Carolina, USA) is regulated by physical and biogeochemical processes on multiple timescales. *PloS One* 8, 1-8. doi: 10.1371/journal.pone.0085117

Kanciruk, P. (1980). Ecology of juvenile and adult *Palinuridae* (spiny lobsters). *Biol. Manage. lobsters* 2, 59–96. doi: 10.1016/B978-0-08-091734-4.50009-3

Kapsenberg, L. and Hofmann, G. E. (2016). Ocean pH time-series and drivers of variability along the northern Channel Islands, California, USA. *Limnology Oceanography* 61, 953–968. doi: 10.1002/lno.10264

Kekuewa, S. A. H. (2020). Seawater CO2-chemistry variability in the near-shore environment of the Southern California Bight. MS thesis, Scripps Institution of Oceanography, University of California San Diego, La Jolla, CA, USA.

Knapp, J. L., Bridges, C. R., Krohn, J., Hoffman, L. C. and Auerswald, L. (2015). Acid–base balance and changes in haemolymph properties of the South African rock lobsters, *Jasus lalandii*, a palinurid decapod, during chronic hypercapnia. *Biochem. Biophys. Res. Commun.* 461, 475–480. doi: 10.1016/j.bbrc.2015.04.025

Kroeker, K. J., Kordas, R. L., Crim, R., Hendriks, I. E., Ramajo, L., Singh, G. S., et al. (2013). Impacts of ocean acidification on marine organisms: quantifying sensitivities and interaction with warming. *Global Change Biol.* 19, 1884–1896. doi: 10.1111/gcb.12179

Kroeker, K. J., Kordas, R. L., Crim, R. N. and Singh, G. G. (2010). Meta-analysis reveals negative yet variable effects of ocean acidification on marine organisms. *Ecol. Lett.* 13, 1419–1434. doi: 10.1111/j.1461-0248.2010.01518.x

Kunkel, J. G. (2013). Modeling the calcium and phosphate mineralization of American lobster cuticle. *Can. J. Fisheries Aquat. Sci.* 70, 1601–1611. doi: 10.1139/cjfas-2013-0034

Kunkel, J. G., Nagel, W. and Jercinovic, M. J. (2012). Mineral fine structure of the American lobster cuticle. *J. Shellfish Res.* 31, 515–526. doi: 10.2983/035.031.0211

Lindberg, R. G. (1955). *Growth, population dynamics, and field behavior in the spiny lobster, Panulirus interruptus (Randall)* (University of California Press, Berkeley, California, United States).

Loflen, C. L. and Hovel, K. A. (2010). Behavioral responses to variable predation risk in the California spiny lobster *Panulirus interruptus*. *Mar. Ecol. Prog. Ser.* 420, 135–144. doi: 10.3354/meps08850

Long, W. C., Swiney, K. M. and Foy, R. J. (2013). Effects of ocean acidification on the embryos and larvae of red king crab, *Paralithodes camtschaticus*. *Mar. pollut. Bull.* 69, 38–47. doi: 10.1016/j.marpolbul.2013.01.011

Lowder, K., Allen, M. C., Day, J. M., Deheyn, D. D., and Taylor, J. R. (2017). Assessment of ocean acidification and warming on the growth, calcification, and biophotonics of a California grass shrimp. *ICES J. Mar. Sci.* 74, 1150–1158. doi: 10.1093/icesjms/fsw246

Lowder, K. (2019). "Integrity of crustacean predator defenses under ocean acidification and warming conditions," in Dissertation (San Diego (CA: University of California San Diego).

Lowder, K., deVries, M. S., Hattingh, R., Day, J. M. D., Andersson, A. J., Zerofski, P., Taylor, J. (2022) Exoskeletal predator defenses of juvenile California spiny lobsters (*Panulirus interruptus*) are affected by fluctuating ocean acidification. PANGAEA, https://doi.org/10.1594/PANGAEA.945362

Lyle, W. G. and MacDonald, C. D. (1983). Molt stage determination in the Hawaiian spiny lobster *Panulirus marginatus*. *J. Crustacean Biol.*, 3, 208–216. doi: 10.2307/1548257

Mangan, S., Urbina, M. A., Findlay, H. S., Wilson, R. W. and Lewis, C. (2017). Fluctuating seawater pH/pCO_2 regimes are more energetically expensive than static pH/pCO_2 levels in the mussel *Mytilus edulis*. *Proc. R. Soc. B* 284, 20171642.

McDonald, M. R., McClintock, J. B., Amsler, C. D., Rittschof, D., Angus, R. A., Orihuela, B., et al. (2009). Effects of ocean acidification over the life history of the barnacle *Amphibalanus amphitrite*. *Mar. Ecol. Prog. Ser.* 385, 179–187. doi: 10.3354/meps08099

McElhany, P. and Busch, D. S. (2013). Appropriate pCO_2 treatments in ocean acidification experiments. *Mar. Biol.* 160, 1807–1812. doi: 10.1007/s00227-012-2052-0

Mehrbach, C., Culberson, C. H., Hawley, J. E. and Pytkowicz, R. M. (1973). Measurement of the apparent dissociation constants of carbonic acid in seawater at atmospheric pressure. *Limnol. Oceanogr.* 18, 897–907. doi: 10.4319/lo.1973.18.6.0897

Melnick, C., Chen, Z. and Mecholsky, J. (1996). Hardness and toughness of exoskeleton material in the stone crab, *Menippe mercenaria*. *J. Materials Res.* 11, 2903–2907. doi: 10.1557/JMR.1996.0367

Menu-Courey, K., Noisette, F., Piedalue, S., Daoud, D., Blair, T., Blier, P. U., et al. (2018). Energy metabolism and survival of the juvenile recruits of the American lobster (*Homarus americanus*) exposed to a gradient of elevated seawater pCO2. *Mar. Environ. Res.* 143, 111-123. doi: 10.1016/j.marenvres.2018.10.002

Newcomb, L. A., Milazzo, M., Hall-Spencer, J. M. and Carrington, E. (2015). Ocean acidification bends the mermaid's wineglass. *Biol. Lett.* 11, 20141075. doi: 10.1098/rsbl.2014.1075

Onitsuka, T., Takami, H., Muraoka, D., Matsumoto, Y., Nakatsubo, A., Kimura, R., et al. (2017). Effects of ocean acidification with pCO_2 diurnal fluctuations on survival and larval shell formation of ezo abalone, *Haliotis discus hannai*. *Mar. Environ. Res.* 134:28-36. doi: 10.1016/j.marenvres.2017.12.015

Ou, M., Hamilton, T. J., Eom, J., Lyall, E. M., Gallup, J., Jiang, A., et al. (2015). Responses of pink salmon to CO_2-induced aquatic acidification. *Nat. Climate Change* 5, 950–955. doi: 10.1038/nclimate2694

Page, H. N., Andersson, A. J., Jokiel, P. L., Ku'ulei, S. R., Lebrato, M., Yeakel, K., et al. (2016). Differential modification of seawater carbonate chemistry by major coral reef benthic communities. *Coral Reefs* 35, 1311–1325. doi: 10.1007/s00338-016-1490-4

Pane, E. F. and Barry, J. P. (2007). Extracellular acid-base regulation during short-term hypercapnia is effective in a shallow-water crab, but ineffective in a deep-sea crab. *Mar. Ecol. Prog. Ser.* 334, 1–9. doi: 10.3354/meps334001

Pierrot, D., Lewis, E. and Wallace, D. (2006). *MS excel program developed for CO_2 system calculations*. doi: 10.3334/CDIAC/otg.CO2SYS_XLS_CDIAC105a

Ptacek, M. B., Sarver, S. K., Childress, M. J. and Herrnkind, W. F. (2001). Molecular phylogeny of the spiny lobster genus Panulirus (Decapoda: Palinuridae). *Mar. Freshw. Res.* 52, 1037–1047. doi: 10.1071/MF01070

Raabe, D., Sachs, C. and Romano, P. (2005). The crustacean exoskeleton as an example of a structurally and mechanically graded biological nanocomposite material. *Acta Materialia* 53, 4281–4292. doi: 10.1016/j.actamat.2005.05.027

Ragagnin, M. N., McCarthy, I. D., Fernandez, W. S., Tschiptschin, A. P. and Turra, A. (2018). Vulnerability of juvenile hermit crabs to reduced seawater pH and shading. *Mar. Environ. Res*. 142:130-140 doi: 10.1016/j.marenvres.2018.10.001

R Core Team (2019). *R: A language and environment for statistical computing* (Vienna, Austria: R Foundation for Statistical Computing). Available at: https://www.R-project.org.

Rosen, M. N., Baran, K. A., Sison, J. N., Steffel, B. V., Long, W. C., Foy, R. J., et al. (2020). Mechanical resistance in decapod claw denticles: Contribution of structure and composition. *Acta Biomaterialia* 110, 196–207. doi: 10.1016/j.actbio.2020.04.037

Ross, E. and Behringer, D. (2019). Changes in temperature, pH, and salinity affect the sheltering responses of Caribbean spiny lobsters to chemosensory cues. *Sci. Rep.* 9, 4375. doi: 10.1038/s41598-019-40832-y

Sachs, C., Fabritius, H., and Raabe, D. (2006). Hardness and elastic properties of dehydrated cuticle from the lobster Homarus americanus obtained by nanoindentation. Journal of Materials Research 21, 1987–1995. doi: 10.1557/JMR.2006.0241

Schofield, R. M. S., Niedbala, J. C., Nesson, M. H., Tao, Y., Shokes, J. E., Scott, R. A., et al. (2009). Br-rich tips of calcified crab claws are less hard but more fracture resistant: a comparison of biomineralized and heavy-element biomaterials. *J. Struct. Biol.* 166, 272–287. doi: 10.1016/j.jsb.2009.01.007

Semesi, I. S., Beer, S. and Björk, M. (2009). Seagrass photosynthesis controls rates of calcification and photosynthesis of calcareous macroalgae in a tropical seagrass meadow. *Mar. Ecol. Prog. Ser.* 382, 41–47. doi: 10.3354/meps07973

Shechter, A., Berman, A., Singer, A., Freiman, A., Grinstein, M., Erez, J., et al. (2008). Reciprocal changes in calcification of the gastrolith and cuticle during the molt cycle of the red claw crayfish *Cherax quadricarinatus*. *Biol. Bull.* 214, 122–134. doi: 10.2307/25066669

Siegel, K., Kaur, M., Grigal, A. C., Metzler, R. and Dickinson, G. (2022). Meta-analysis suggests variable, but pCO_2-specific, effects of ocean acidification on crustacean biomaterials. *Ecol. Evol.* 12 (6), e8922. doi: 10.22541/au.164370924.40403866/v1

Silbiger, N. J. and Sorte, C. J. (2018). Biophysical feedbacks mediate carbonate chemistry in coastal ecosystems across spatiotemporal gradients. *Sci. Rep.* 8, 796. doi: 10.1038/s41598-017-18736-6

Small, D. P., Calosi, P., Boothroyd, D., Widdicombe, S. and Spicer, J. I. (2016). The sensitivity of the early benthic juvenile stage of the European lobster *Homarus gammarus* (L.) to elevated pCO_2 and temperature. *Mar. Biol.* 163, 1–12. doi: 10.1007/s00227-016-2834-x

Spanier, E. and Zimmer-Faust, R. K. (1988). Some physical properties of shelter that influence den preference in spiny lobsters. *J. Exp. Mar. Biol. Ecol.* 121, 137–149. doi: 10.1016/0022-0981(88)90251-1

Spicer, J. I., Raffo, A. and Widdicombe, S. (2007). Influence of CO_2- related seawater acidification on extracellular acid–base balance in the velvet swimming crab *Necora puber*. *Mar. Biol.* 151, 1117–1125. doi: 10.1007/s00227-006-0551-6

Takeshita, Y., Frieder, C., Martz, T., Ballard, J., Feely, R., Kram, S., et al. (2015). Including high-frequency variability in coastal ocean acidification projections. *Biogeosciences* 12, 5853–5870. doi: 10.5194/bg-12-5853-2015

Tarsitano, S., Lavalli, K., Horne, F. and Spanier, E. (2006). The constructional properties of the exoskeleton of homarid, palinurid, and scyllarid lobsters. *Issues Decapod Crustacean Biol.*, 557, 9–20. doi: 10.1007/1-4020-4756-8_3

Taylor, J. R., and Kier, W. M. (2006). A pneumo-hydrostatic skeleton in land crabs. *Nature* 440, 1005–1005. doi: 10.1038/4401005a

Taylor, J. R. A., Gilleard, J. M., Allen, M. C. and Deheyn, D. D. (2015). Effects of CO_2-induced pH reduction on the exoskeleton structure and biophotonic properties of the shrimp *Lysmata californica*. *Sci. Rep.* 5, 10608. doi: 10.1038/srep10608

Travis, D. F. (1954). The molting cycle of the spiny lobster, *Panulirus argus* latreille. i. molting and growth in laboratory-maintained individuals. *Biol. Bull.* 107, 433–450. doi: 10.2307/1538591

Travis, D. F. (1963). Structural features of mineralization from tissue to macromolecular levels of organization in the decapod Crustacea. *Ann. New York Acad. Sci.* 109, 177–245. doi: 10.1111/j.1749-6632.1963.tb13467.x

Truchot, J. (1979). Mechanisms of the compensation of blood respiratory acid-base disturbances in the shore crab, *Carcinus maenas* (L.). *J. Exp. Zoology* 210, 407–416. doi: 10.1002/jez.1402100305

Tukey, J. W. (1977). *Exploratory data analysis* (Reading, Mass: Addison-Wesley Publishing Company).

Uppström, L. R. (1974). The boron/chlorinity ratio of deep-sea water from the Pacific Ocean. *Deep Sea Res. Oceanographic Abstracts (Elsevier)*, 21:161–162. doi: 10.1016/0011-7471(74)90074-6

Vigh, D. A. and Dendinger, J. E. (1982). Temporal relationships of postmolt deposition of calcium, magnesium, chitin and protein in the cuticle of the Atlantic blue crab, *Callinectes sapidus* Rathbun. *Comp. Biochem. Physiol. Part A: Physiol.* 72, 365–369. doi: 10.1016/0300-9629(82)90232-8

Wahl, M., Saderne, V. and Sawall, Y. (2015). How good are we at assessing the impact of ocean acidification in coastal systems? limitations, omissions and strengths of commonly used experimental approaches with special emphasis on the neglected role of fluctuations. *Mar. Freshw. Res.* 67, 25–36. doi: 10.1071/MF14154

Wahl, M., Schneider Covachã, S., Saderne, V., Hiebenthal, C., Müller, J., Pansch, C., et al. (2018). Macroalgae may mitigate ocean acidification effects on mussel calcification by increasing pH and its fluctuations. *Limnology Oceanography* 63, 3–21. doi: 10.1002/lno.10608

Weaver, J. C., Milliron, G. W., Miserez, A., Evans-Lutterodt, K., Herrera, S., Gallana, I., et al. (2012). The stomatopod dactyl club: a formidable damage-tolerant biological hammer. *Science* 336, 1275–1280. doi: 10.1126/science.1218764

Whiteley, N. M. (2011). Physiological and ecological responses of crustaceans to ocean acidification. *Mar. Ecol. Prog. Ser.* 430, 257–271. doi: 10.3354/meps09185

Whiteley, N. M., Suckling, C. C., Ciotti, B. J., Brown, J., McCarthy, I. D., Gimenez, L., et al. (2018). Sensitivity to near-future CO_2 conditions in marine crabs depends on their compensatory capacities for salinity change. *Sci. Rep.* 8, 15639. doi: 10.1038/s41598-018-34089-0

Wickham, H. (2016a). *ggplot2: elegant graphics for data analysis*. 2nd ed. (New York: Springer International Publishing).

Wickham, H. (2016b). *Tidyr: Easily tidy data with spread () and gather () functions. version 0.6.0.*

Wickham, H. (2017). "Forcats: Tools for working with categorical variables (factors)," in *R package version 0.2. 0.* Available at: https://CRAN.R-project.org/package=forcats.